Meteoritics & Planetary Science 39, Nr 1, 117–135 (2004)
Abstract available online at http://meteoritics.org

Noble gases in chondrules and associated metal-sulfide-rich samples: Clues on chondrule formation and the behavior of noble gas carrier phases

Nadia VOGEL,[1†*] Ingo LEYA,[1] Addi BISCHOFF,[2] Heinrich BAUR,[1] and Rainer WIELER[1]

[1]Institute for Isotope Geology and Mineral Resources, Sonneggstrasse 5, NO C61, ETH Zürich, 8092 Zürich, Switzerland
[2]Institute of Planetology, Wilhelm-Klemm-Str. 10, University of Münster, 48149 Münster, Germany
[†]Present address: Berkeley Geochronology Center, 2455 Ridge Road, Berkeley, California 94709, USA
[*]Corresponding author. E-mail: nvogel@bgc.org

(Received 23 June 2002; revision accepted 4 December 2003)

Abstract–Chondrules are generally believed to have lost most or all of their trapped noble gases during their formation. We tested this assumption by measuring He, Ne, and Ar in chondrules of the carbonaceous chondrites Allende (CV3), Leoville (CV3), Renazzo (CR2), and the ordinary chondrites Semarkona (LL3.0), Bishunpur (LL3.1), and Krymka (LL3.1). Additionally, metal-sulfide-rich chondrule coatings were measured that probably formed from chondrule metal. Low primordial ^{20}Ne concentrations are present in some chondrules, while even most of them contain small amounts of primordial ^{36}Ar. Our preferred interpretation is that—in contrast to CAIs—the heating of the chondrule precursor during chondrule formation was not intense enough to expel primordial noble gases quantitatively. Those chondrules containing both primordial ^{20}Ne and ^{36}Ar show low presolar-diamond-like ^{36}Ar/^{20}Ne ratios. In contrast, the metal-sulfide-rich coatings generally show higher gas concentrations and Q-like ^{36}Ar/^{20}Ne ratios. We propose that during metal-silicate fractionation in the course of chondrule formation, the Ar-carrying phase Q became enriched in the metal-sulfide-rich chondrule coatings. In the silicate chondrule interior, only the most stable Ne-carrying presolar diamonds survived the melting event leading to the low observed ^{36}Ar/^{20}Ne ratios. The chondrules studied here do not show evidence for substantial amounts of fractionated solar-type noble gases from a strong solar wind irradiation of the chondrule precursor material as postulated by others for the chondrules of an enstatite chondrite.

INTRODUCTION

Chondrules are small silicate spherules in primitive meteorites that show evidence for a once molten stage. Although they are common in most chondrite groups (e.g., Brearley and Jones 1998), their formation mechanism(s) and environment(s) are uncertain. The two main theories are nebular chondrule formation by melting of dust-ball precursors and chondrule formation in a planetary environment (see, e.g., Brearley and Jones [1998] and Rubin [2000] for comprehensive reviews about chondrule formation and heating models).

Previous noble gas studies on chondrules revealed low to zero noble gas concentrations apart from cosmogenic gases (Kim and Marti 1994; Miura and Nagao 1996; Nakamura et al. 1999; Okazaki et al. 2001a; Smith et al. 1977, Swindle et al. 1991). This is generally attributed to extensive gas loss during melting of a more gas-rich precursor (Alexander 1989; Connolly et al. 2001; Kong and Ebihara 1997; Kong and Palme 1999; Scott and Taylor 1983). However, Okazaki et al. (2001b) reported high noble gas concentrations (e.g., up to 7 × 10^{-6} cm^{3}STP/g ^{36}Ar) in chondrules of the enstatite chondrite Yamato (Y)-791790. These chondrules are surrounded by matrix with lower gas concentrations (e.g., ~4 × 10^{-7} cm^{3}STP/g ^{36}Ar). The authors explained the high noble gas concentrations in the chondrules by irradiation of their precursor material with solar wind (SW) noble gases from the young sun. These noble gases were fractionated toward a composition depleted in He and Ne, probably during melting of the irradiated precursor dust. Then, the chondrules were transported to distant nebular regions where they accreted to the enstatite parent body. Okazaki et al. (2001b) argue that their finding supports the X-wind model proposed by Shu et al. (1997, 2001), in which chondrules were formed close to the sun and subsequently were ejected to the present-day asteroid belt.

If processing of material through the X-wind region was indeed a major chondrule forming process, primordial solar-

like noble gases might also be expected in chondrules of other meteorite classes, unless this process was restricted to chondrules found today in enstatite chondrites.

Therefore, we measured He, Ne, and Ar in chondrules of the carbonaceous chondrites Allende (CV3), Leoville (CV3), and Renazzo (CR2), and the ordinary chondrites Semarkona (LL3.0), Bishunpur (LL3.1), and Krymka (LL3.1). Helium-3 and ^{4}He are mainly cosmogenic and radiogenic, respectively, and thus, are not reported here. Kr and Xe concentrations in some chondrules were indistinguishable from blank values and, therefore, not measured routinely. The study also includes metal-sulfide (MS)-rich coatings of chondrules, MS droplets within chondrules, and MS-rich patches in the matrix that are also genetically related to chondrules (Alexander 1989; Connolly et al. 1994, 2001; Kong and Ebihara 1997; Kong and Palme 1999). We assume that, during chondrule formation, small MS droplets segregated from the silicate melt, migrated to the chondrule margins, and were eventually expelled (e.g., Connolly et al. 2001; Kong and Palme 1999). Expelled droplets formed coatings around chondrules or were completely separated from their host chondrules and are now present as isolated MS-rich patches within the matrices of primitive chondrites. It is also possible that MS evaporated from, and subsequently recondensed back onto, chondrule surfaces (e.g., Connolly et al. 2001). Alternatively, Kojima et al. (2003) discuss the extraction of chondrule MS and the formation of the coatings during later impact events on the parent bodies to which the chondrules first assembled. Due to the genetic link between chondrules and MS, a comparison of noble gas data from both constituents is crucial to understanding their noble gas signatures. The data will also be related to the data of samples of fine-grained rims and matrix (collectively called "matrix" hereafter) of the respective meteorites (Vogel et al. 2003) to draw conclusions on possible chondrule precursor materials and to understand the behavior of the noble gas carrier phases during chondrule formation.

NOBLE GAS RESERVOIRS, SAMPLES, AND EXPERIMENTAL PROCEDURE

Noble Gases in Unequilibrated Chondrites

The bulk noble gas composition of a primitive meteorite generally represents a mixture of different components. These were either trapped in the accreting bodies of the solar system or later produced in situ. We will discuss which component dominates the noble gas composition of the chondrules. Therefore, we introduce the components in some detail in the following and give relevant Ne and Ar isotopic and elemental compositions in Table 1.

Two of the major trapped noble gas components reside in specific carrier phases mainly found in the matrices of unequilibrated chondrites (Huss et al. 1996; Smith et al. 1977). Presolar diamonds carry mainly He and Ne but also contain the isotopically "anomalous" Xe-HL component (Huss and Lewis 1994a). The carbonaceous phase Q (Lewis et al. 1975; Ott et al. 1981; Busemann et al. 2000) is less depleted in Ar, Kr, and Xe than in He and Ne compared to solar composition and shows "normal" isotopic compositions (Lewis et al. 1975; Ott 2002). HL and Q gases were trapped very early in the history of the meteorites and, thus, are called "primordial." In contrast, SW noble gases usually do not deserve this attribute because they were trapped possibly much later, upon irradiation of dust by the solar wind on asteroidal and/or planetary surfaces. Some of this dust became compacted and formed what are now called gas-rich meteorites. However, Busemann et al. (2003) recently showed that the enstatite chondrite St. Mark's contains solar noble gases of primordial origin, i.e., trapped before parent body formation. The authors show that the previously postulated "subsolar" noble gas component particularly prominent in many E chondrites (Crabb and Anders 1981) is, thus, not a bona fide primordial noble gas component but a mixture of primordial solar gases, Q gases, and atmospheric contamination.

Table 1. Ne and Ar isotopic and elemental compositions of various noble gas reservoirs relevant in this study.[a]

	^{20}Ne/^{22}Ne	^{21}Ne/^{22}Ne	^{36}Ar/^{38}Ar	^{36}Ar/^{20}Ne
Q	10.05(5)–10.7(2)[b]	0.0291(16)–0.0294(10)[b]	5.34(2)[b]	14–84[b]
HL	8.50(6)[c]	0.036(1)[c]	4.41(6)[c]	0.103(42)[c]
SW	13.8(1)[d]	0.0328(5)[d]	5.58(3)[d]	~0.04[d]
GCR	0.70–0.93[e]	0.80–0.95[e]	0.65(3)[e]	–
Air	9.80(8)[f]	0.0290(3)[f]	5.32(1)[g]	1.9[h]

[a]Numbers in parentheses represent uncertainties in units of the least significant digits.
[b]Busemann et al. (2000).
[c]Huss and Lewis (1994a).
[d]Benkert et al. (1993).
[e]Galactic cosmic radiation (chondritic); Wieler (2002).
[f]Eberhardt et al. (1965).
[g]Nier (1950).
[h]Ozima and Podosek (2002).

The in situ-produced noble gases have either a radiogenic or cosmogenic origin. Radiogenic gases, e.g., ^{4}He and ^{40}Ar, result from the decay of the radionuclides $^{235, 238}$U, ^{232}Th, and ^{40}K, while cosmogenic noble gases are produced by nuclear reactions induced by galactic cosmic radiation (GCR) on meteoritic target material.

Sample Selection

The studied meteorites are listed in Table 2. They had to fulfill several requirements. Only type 2 and 3 chondrites were selected to minimize losses or redistribution of trapped noble gases due to secondary thermal alteration. Regolith breccias were excluded, since implanted SW noble gases could have obscured possible primordial solar signatures in the chondrules. To minimize cosmogenic contributions, the exposure ages of the samples had to be as short as possible. This criterion is not fulfilled by Krymka, which has an exposure age of ~25 Ma. Nevertheless, we included Krymka because it is among the most unequilibrated chondrites available and is mineralogically/petrographically well-investigated (Huang et al. 1996; Rambaldi and Wasson 1984; Semenenko et al. 2001). Finally, the chondrules had to be large enough for a proper hand separation. This precluded CM chondrites.

Most of the cut and polished meteorite chips were mapped with a CamScan CS44LB SEM (Fig. 1). To avoid carbon contamination, the chips were not coated. Then, small chondrule and MS-rich samples were carefully separated under a binocular microscope. Most of the chondrules were porphyritic, and some of the Bishunpur chondrules could be additionally subclassified (see Table A1). Special attention was paid to avoid cross-contamination of the samples with surrounding fine-grained and generally more gas-rich matrix (Nakamura et al. 1999; Vogel 2003; Vogel et al. 2003) and MS-rich material. Note that the MS-rich coatings themselves often contain a certain degree of intimately admixed matrix-like silicate material (e.g., dark lumps in the MS-rich sample "B-MSC-A" in Fig. 1d; or, e.g., Alexander 1989).

The samples are labelled as follows: the first letter indicates the meteorite (A = Allende, L = Leoville, S = Semarkona, B = Bishunpur, K = Krymka, R = Renazzo) followed by the specification of the constituent (Ch = Chondrule; MSD = MS-droplet; MSC = MS-rich coating; MS = MS-rich sample, where a specification as droplet or coating was not possible on the basis of the SEM image; see Fig. 1c). The next letter (A–K) distinguishes different samples of the same constituent; the numbers (1–7) attached to these letters indicate different analyses of the same object.

Gas Extraction, Measurements, Data Reduction

Losely bound atmospheric noble gases were removed by baking the samples in a vacuum (24 hr, 100 °C) before noble gases were extracted by melting the samples (generally for 1 to 3 min) with a Nd-YAG-laser in CW mode. For a detailed description of the noble gas extraction technique, gas purification, spectrometer settings, interference corrections, and the calibration procedure, see Vogel et al. (2003).

Blanks

Due to the generally low gas concentrations in the chondrule samples, a precise blank correction was important. Therefore, we measured 3 types of blanks (also described in Vogel et al. [2003]). Cold blanks simulated a sample extraction procedure without a laser beam and were used to determine the variability of the blanks over time. Sample and aliminium blanks were measured to control the completeness of the noble gas extraction from the samples and to correct them for blank contributions. Sample and aluminium blanks

Table 2. Estimated $^{36}Ar_{nc}$ contributions to $^{36}Ar_{tr}$ concentrations of the studied meteorites.

	Average chondrule $(^{22}Ne/^{21}Ne)_{cos}$	Max. shielding depth[a]	Exposure age[b]	Average bulk Cl concentration (ppm)[c]	Upper limit $^{36}Ar_{nc}$ concentration (cm^3STP/g)[d]	Average $^{36}Ar_{tr}$ of chondrules (cm^3STP/g)	Proportion of upper limit $^{36}Ar_{nc}$ at $^{36}Ar_{tr}$ (%)[e]
Allende (CV3)	1.06	60	5.1	270	1.48E–09	1.70E–08	9
Leoville (CV3)	1.08	50	9.7	–	2.56E–09	4.70E–09	55
Renazzo (CR2)	1.15	10	6.1	–	4.03E–10	6.40E–09	6
Semarkona (LL3.0)	1.15	10	9.1	130	2.89E–10	2.33E–08	1
Bishunpur (LL3.1)	1.11	25	10.7	–	8.16E–10	1.22E–08	7
Krymka (LL3.1)	1.09	50	26.3	–	3.34E–09	1.19E–08	28

[a]The maximum shielding depth for each meteorite was estimated from Fig. 14 in Leya et al. (2000) on the basis of average chondrule $(^{22}Ne/^{21}Ne)_{cos}$ ratios assuming that the latter mainly reflect shielding conditions. This is supported by similar $(^{22}Ne/^{21}Ne)_{cos}$ ratios calculated from bulk Ne data of the respective meteorites (Schultz and Frank 2000).

[b]The exposure ages were estimated via bulk $^{21}Ne_{cos}$ concentrations (data source: Shultz and Frank 2000), a typical $(^{22}Ne/^{21}Ne)^{cos}$ of 1.11 (Wieler 2002), and $^{21}Ne_{cos}$ production rates were calculated according to Eugster (1988).

[c]Estimate based on bulk cabonaceous and ordinary chondrite Cl concentrations of Mason (1979) since chondrule Cl concentrations for chondrules of the meteorites studied here were not available.

[d]Exposure-depth-dependent $^{36}Ar_{nc}$ production rates (upper limits) are estimated by I. Leya. Compared to bulk, Cl concentrations in chondrules are assumed to be depleted by a factor of 5. See text for further explanation.

[e]Contributions of upper limits of $^{36}Ar_{nc}$ to average $^{36}Ar_{tr}$ concentrations of chondrules for a Cl-depletion factor of 5.

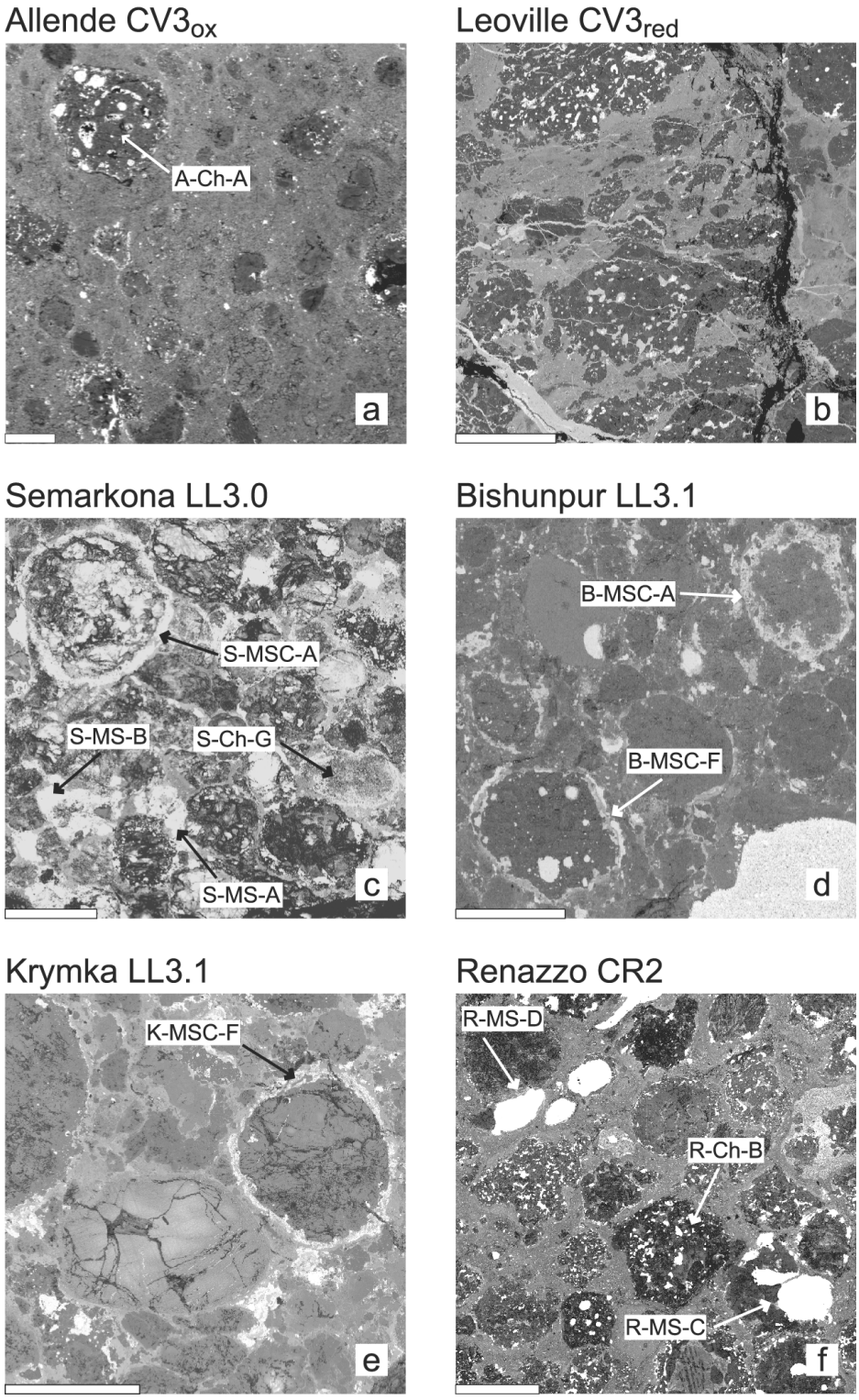

Fig. 1. Backscattered electron images of the chondrites Allende (CV3, oxidised subgroup), Leoville (CV3, reduced subgroup), Semarkona (LL3.0), Bishunpur (LL3.1), Krymka (LL3.1), and Renazzo (CR2). Selected sample locations are indicated by arrows. Spheroidal chondrules are embedded in fine-grained matrix for Allende, Leoville, and Renazzo. Matrix of the ordinary chondrites is mainly restricted to interstices between chondrules. Studied chondrules of Allende and Leoville do not contain metal-sulfide-rich coatings, while chondrules of the ordinary chondrites are often surrounded by them (bright chondrule coatings). The large bright patch in the lower right corner of (d) is conductive silver. Metal-sulfide in Renazzo often occurs as large droplets within chondrules or isolated in the matrix. The lengths of the bars are 1 mm.

were determined by re-extracting the already degassed samples and by firing the laser on the aluminium sample holder, respectively. Thereby, extraction times and laser energies similar to the values of the respective sample runs were used. Sample blanks were used for the blank correction except in those cases where they released discernible amounts of sample gas, i.e., where the gas concentrations of the sample blanks exceeded those of adjacent aluminium blanks. This additional sample gas was then added to the noble gas amounts of the nominal sample extraction step after both had been corrected with an aluminium (or eventually cold) blank.

Average long-term ^{20}Ne and ^{36}Ar cold blanks were low, $(1.1 \pm 0.6) \times 10^{-13}$ and $(1.4 \pm 0.7) \times 10^{-13}$ cm^{3}STP, respectively, and roughly of atmospheric composition. The variability for both blanks within one run was in the range of 15% only. While this variability is similar to the statistical uncertainty of individual ^{20}Ne blanks, it distinctly exceeded the statistical uncertainty of a single ^{36}Ar blank. Therefore, ^{20}Ne blanks used for the blank correction could be applied with their respective statistical uncertainties, but for all ^{36}Ar blanks, we adopted an uncertainty of 15%.

The ^{20}Ne and ^{36}Ar blanks contributed on average ~4% and ~16% to the measured gas concentrations, respectively. Only for some very small and/or gas-poor chondrules, both blanks increased to up to 70%.

RESULTS: CHONDRULES

Table A1 shows the blank-corrected Ne and Ar concentrations and isotopic compositions of the chondrules. Where available, elemental ratios corrected for cosmogenic contributions are given. For the sake of clarity, we added the subscript "tr" (=trapped) to the non-cosmogenic noble gas data ($^{20}Ne_{tr}$, $^{36}Ar_{tr}$, $[^{36}Ar/^{20}Ne]_{tr}$). We will show later that this non-cosmogenic portion can neither be attributed to an underestimated blank nor to atmospheric contamination of our samples, and thus, the subscript "tr" is justified. Finally, Table A1 gives the contributions of the ^{20}Ne and ^{36}Ar blanks to the trapped noble gas concentrations before the blank correction. The corrections for cosmogenic contributions are described in the following sections.

Correction of ^{20}Ne for Cosmogenic Contributions

For typical chondritic material, the cosmogenic ^{20}Ne/^{21}Ne ratio is in the range of 0.88–0.98, depending on the chemistry and the shielding depth of a given sample (Leya et al. 2000; Wieler 2002). The addition of even small trapped noble gas amounts shifts this ratio to distinctly higher values (see Table 1). However, because of the variability of the cosmogenic ^{20}Ne/^{21}Ne ratio, it is often difficult to decide whether a slightly higher than "average cosmogenic" ^{20}Ne/^{21}Ne ratio in a chondrule sample is really due to a small non-cosmogenic contribution. This is illustrated in Fig. 2, where the ratios ^{22}Ne/^{21}Ne versus ^{20}Ne/^{21}Ne of our chondrules (black symbols) are plotted together with data from bulk ordinary chondrites (gray symbols) of high petrographic types (5 and 6), simple exposure histories, and exposure ages >30 Ma, as compiled by Schultz and Franke (2000). These meteorites are expected to contain a very low proportion of non-cosmogenic Ne. The data display a well-defined left-hand margin that can approximately be described by a straight line. We interpret this line to represent the "OCNL" (Ordinary chondrite cosmogenic Ne line). In these plots, small amounts of trapped Ne lead to deviations toward the right of the OCNL. The OCNL has a positive slope, i.e., the ^{20}Ne/^{21}Ne ratios increase slightly with increasing ^{22}Ne/^{21}Ne. This reflects the dependence of the isotopic composition of cosmogenic Ne from shielding depth and chemistry of a sample. The slope of the OCNL is in good agreement with the data predicted from model calculations for bulk chondrites (Leya et al. 2000).

We can apply the OCNL to our chondrules because chondrules and bulk ordinary chondrites generally contain similar proportions of Mg, Al, and Si, the main target elements for cosmogenic Ne production (chemical data for bulk ordinary chondrites from Mason [1979] and for chondrule populations from McSween et al. [1983]). The model by Leya et al. (2000) predicts that, e.g., the cosmogenic ^{20}Ne/^{21}Ne ratios of chondrules and ordinary chondrites agree to within 1% despite their different chemical compositions.

Most of the chondrules plot on the right-hand side of the OCNL. This suggests the presence of non-cosmogenic noble gases, even though, for many data points, the deviation from the OCNL is smaller than their 1σ uncertainty. Note that only very few data points plot on the left-hand side of the OCNL. With one exception, all these points agree with the OCNL within their 1σ uncertainties. This is a further argument that at least those samples plotting to the right of the OCNL by more than 1σ, but presumably also some of the others, indeed contain small amounts of trapped Ne. We calculated these trapped ^{20}Ne ($^{20}Ne_{tr}$) amounts based on a cosmogenic ^{20}Ne/^{21}Ne ratio deduced individually for every chondrule. The cosmogenic ^{20}Ne/^{21}Ne ratio was determined as the intersection of the OCNL with a line defined by the data point of the respective chondrule and a trapped end member (see Fig. 2a). For a trapped end member, we adopted the Ne isotopic composition of presolar diamonds (Table 1), but this assumption is not crucial.

Trapped ^{20}Ne

The concentrations of $^{20}Ne_{tr}$ are generally low ($\leq 2 \times 10^{-8}$ cm^{3}STP/g; Table A1). Values consistent with zero within 1σ uncertainties are given in italics. Fifteen among the 50 chondrule samples show $^{20}Ne_{tr}$ concentrations above zero by more than 1σ. The blank contributions to these $^{20}Ne_{tr}$

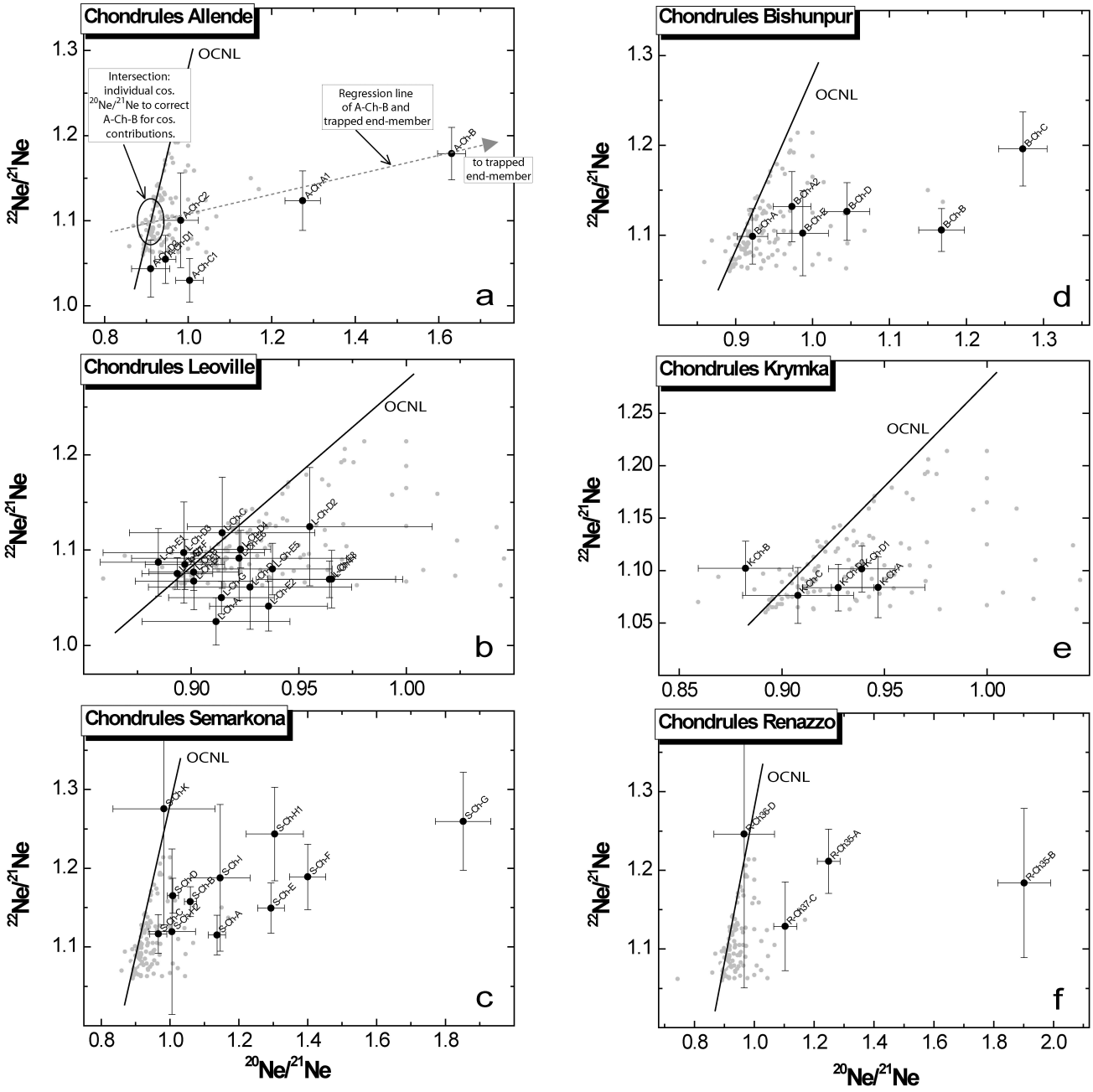

Fig. 2. $^{20}Ne/^{21}Ne$ versus $^{22}Ne/^{21}Ne$ ratios of chondrules (black symbols) of the 6 meteorites studied. Also plotted are bulk ordinary chondrite data (gray symbols) with very low trapped and high cosmogenic noble gas concentrations. Their left-hand envelope defines the ordinary chondrite cosmogenic Ne isotopic composition (OCNL), taking into account the variability of the sample chemistry but mainly of the shielding depth. Most of the chondrules lie at the right-hand side of the OCNL, indicating the presence of non-cosmogenic ^{20}Ne. Chondrule data were corrected for cosmogenic contributions with individual $^{20}Ne/^{21}Ne$ ratios obtained by calculating the intersection of the OCNL with an extended regression line between the respective chondrule and a trapped end member (see diagram 2a). Data points lying at the left-hand side of the OCNL display nominally negative corrected ^{20}Ne concentrations (see Table A1). Error bars are 1σ. See text for further explanation.

concentrations do not exceed 16%. Thus, the $^{20}Ne_{tr}$ concentrations of these samples cannot be attributed to underestimated blanks. However, below we use the $(^{36}Ar/^{20}Ne)_{tr}$ ratios to test whether the samples may be affected by residual adsorbed atmospheric Ne or by matrix or MS contamination.

Correction of the Measured ^{36}Ar for Cosmogenic Contributions

In contrast to Ne, where 3 isotopes are available, only the $^{36}Ar/^{38}Ar$ ratio can be used to correct for cosmogenic Ar, since ^{40}Ar is mainly radiogenic. Fortunately, the cosmogenic

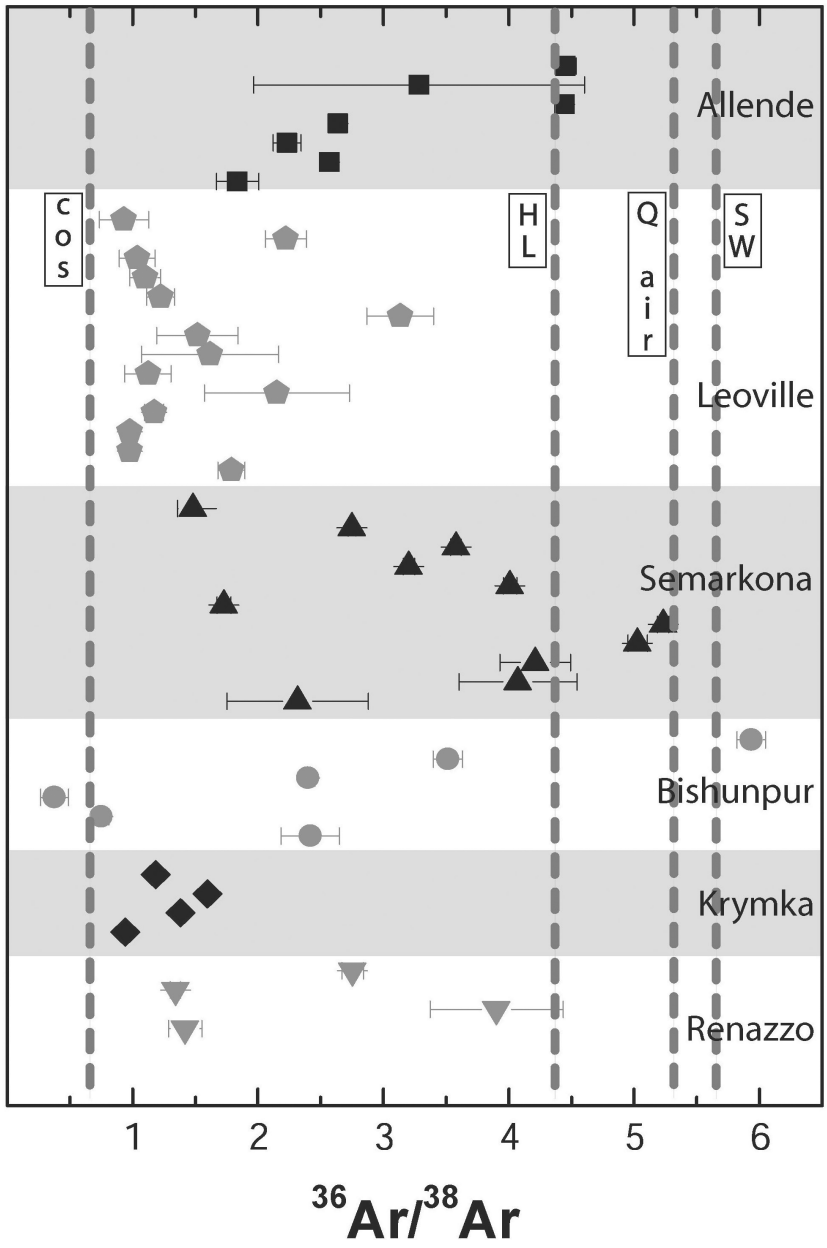

Fig. 3. $^{36}Ar/^{38}Ar$ ratios of all studied chondrules. All but 2 Bishunpur chondrules plot to the right of the cosmogenic $^{36}Ar/^{38}Ar$ ratio of 0.65 ± 0.03, indicating the presence of non-cosmogenic ^{36}Ar. Most $^{36}Ar/^{38}Ar$ ratios scatter between cosmogenic and presolar diamond compositions. Two Semarkona chondrules in the range of $^{36}Ar/^{38}Ar$ ratios of phase Q are contaminated with matrix (see text for explanation). We cannot explain the unusually high and low $^{36}Ar/^{38}Ar$ ratios of 2 Bishunpur samples, respectively. For the cosmogenic correction of ^{36}Ar, we used the cosmogenic $^{36}Ar/^{38}Ar$ ratio given above and the trapped end member of phase Q with a $^{36}Ar/^{38}Ar$ ratio of 5.34 ± 0.02 (see Table 1). Error bars are 1σ.

$^{36}Ar/^{38}Ar$ ratio is nearly identical for Ca and Fe, the 2 main target elements for cosmogenic Ar production (Wieler 2002). Therefore, a uniform cosmogenic $^{36}Ar/^{38}Ar$ ratio of 0.65 ± 0.03 was adopted for all chondrules. Figure 3 shows the $^{36}Ar/^{38}Ar$ ratios of the measured chondrules. Most of the data points lie to the right of the cosmogenic $^{36}Ar/^{38}Ar$ ratio, indicating the presence of non-cosmogenic ^{36}Ar ($^{36}Ar_{tr}$). The samples were corrected for cosmogenic contributions by a 2-component deconvolution. For a non-cosmogenic end member, we adopted the $^{36}Ar/^{38}Ar$ ratio of phase Q (5.34 ± 0.02; Table 1), the major Ar-carrier phase in unequilibrated chondrites. Even adopting pure Ar-HL in presolar diamonds (Table 1) would not appreciably change, e.g., the noble gas pattern in Fig. 4.

Cosmogenic ^{36}Ar can also be produced by neutron-capture on ^{35}Cl and subsequent β^--decay ($^{36}Ar_{nc}$). This contribution strongly depends on the preatmospheric size of the meteoroid and the shielding depth of the sample and is

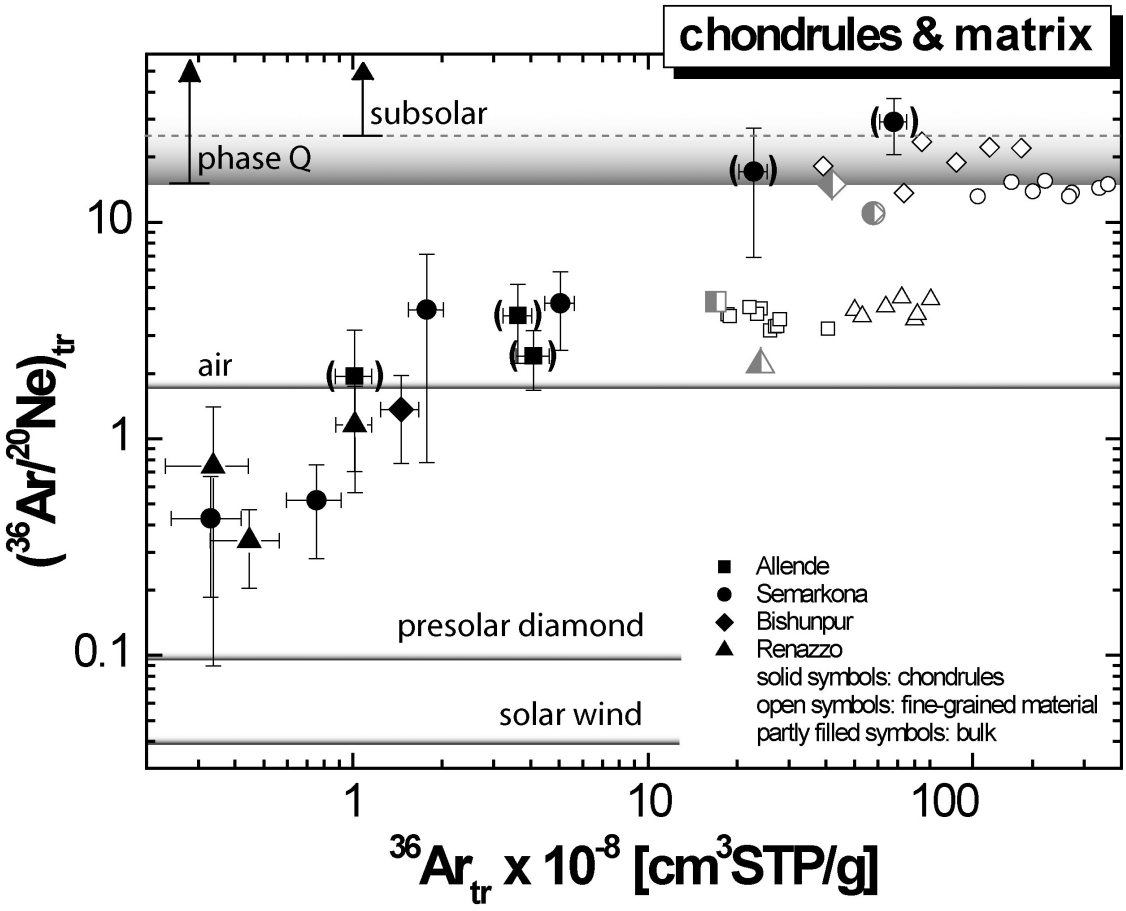

Fig. 4. $(^{36}Ar/^{20}Ne)_{tr}$ ratios versus $^{36}Ar_{tr}$ concentrations of Allende, Semarkona, Bishunpur, and Renazzo chondrules (solid symbols). Also shown are matrix data (open symbols; see Vogel et al. 2003) and bulk values (partly filled symbols; Schultz and Franke 2000) of the respective meteorites without error bars. Data points of chondrules possibly contaminated with matrix or surrounding MS (in the case of sample S-Ch-G) are shown in brackets. A "subsolar" $^{36}Ar/^{20}Ne$ range (Busemann et al. 2002) is indicated to enable a comparison with the chondrule data of Okazaki et al. (2001b) displaying this noble gas signature. Chondrules generally show lower $(^{36}Ar/^{20}Ne)_{tr}$ ratios as well as lower $^{36}Ar_{tr}$ concentrations than the respective matrices. This could point to a presolar diamond or solar-like signature in the chondrules (see text for further explanation). Error bars are 1σ.

generally negligible compared to $^{36}Ar_{tr}$ concentrations in bulk unequilibrated chondrites (see, e.g., Vogel 2003). This might not be true for chondrules due to their low $^{36}Ar_{tr}$ concentrations, although we can expect Cl to be depleted in chondrules. Unfortunately, Cl concentration data for chondrules of the meteorites studied here are lacking. Therefore, we use bulk carbonaceous and ordinary chondrite Cl values (Mason 1979) and conservatively assume a depletion factor of 5 for the highly volatile Cl in chondrules relative to bulk chondrites. This corresponds to an upper limit of depletion of the moderately volatile Na in chondrules (e.g., Huang et al. 1996; Grossman et al. 1988) and is in broad agreement with Cl concentrations given for chondrules of the LL3 chondrite Chainpur (Swindle et al. 1991). The size- and shielding-dependent $^{36}Ar_{nc}$ production rates are calculated using the model described by Leya et al. (2000). Table 2 gives the upper limits for the modeled $^{36}Ar_{nc}$ amounts and their estimated contributions to the average $^{36}Ar_{tr}$ concentrations of the chondrules. We point out again that these figures are conservative upper limits because the Cl depletion in chondrules will probably be higher than a factor of 5. Furthermore, the estimate of the $^{36}Ar_{nc}$ production rate assumes maximum production in a meteoroid of a given size range, which is a conservative estimate also. The modeled upper limits for $^{36}Ar_{nc}$ limits would indeed compromise the data for Leoville and Krymka chondrules. More importantly, however, the possible corrections are negligible for the chondrules of the meteorites used to discuss the origin of the noble gases in chondrules (see, e.g., Fig. 4).

Trapped ^{36}Ar

Concentrations of $^{36}Ar_{tr}$ clearly above zero by more than 1σ could be detected in 43 out of the 47 chondrule samples measured for Ar. The concentrations range up to 5×10^{-8} cm^3STP/g; exceptions are 2 Semarkona chondrules (S-Ch-

H1, S-Ch-G) with $^{36}Ar_{tr}$ concentrations as high as 10^{-7} cm^3STP/g most probably resulting from contamination with matrix or MS-rich material (see below). For 3 of the 44 samples, the ^{36}Ar blank contributes more than 50% to the $^{36}Ar_{tr}$. In these cases, we cannot exclude that a slightly underestimated blank considerably affects the $^{36}Ar_{tr}$ data. Therefore, these data are not considered any further. For those samples containing both $^{20}Ne_{tr}$ and $^{36}Ar_{tr}$ the possibility that the trapped gas concentrations may be influenced by adsorbed air or matrix/MS-contamination is addressed based on the $(^{36}Ar/^{20}Ne)_{tr}$ ratios.

$^{36}Ar/^{20}Ne$ Ratios of the Trapped Component in Chondrules

Thirteen chondrule samples unequivocally show both $^{20}Ne_{tr}$ and $^{36}Ar^{tr}$. The $(^{36}Ar/^{20}Ne)_{tr}$ ratios (Table A1) are shown in Fig. 4 as a function of the $^{36}Ar_{tr}$ concentrations. Also plotted are matrix data of the respective meteorites (Vogel et al. 2003). Matrix-like material is a probable chondrule precursor (e.g., Alexander 1989; Connolly et al. 2001; Kong and Ebihara 1997; Kong and Palme 1999; Scott and Taylor 1983) but also represents a possible source of contamination for the chondrule samples. Compared to the gas-rich matrix, the major part of the chondrules shows low $^{36}Ar_{tr}$ concentrations (with few exceptions in the range of or below 1% of matrix $^{36}Ar_{tr}$) and low $(^{36}Ar/^{20}Ne)_{tr}$ ratios. The latter could indicate mixtures between matrix-like noble gases, with a noble gas component having a distinctly lower $^{36}Ar/^{20}Ne$ ratio, such as HL or SW noble gases. Also, pure HL or slightly mass fractionated SW noble gases might be possible. However, first we discard those samples that might have been significantly contaminated with matrix or MS, which also show matrix-like or higher $(^{36}Ar/^{20}Ne)_{tr}$ ratios (see below), during sample separation. We will further exclude that adsorbed air is the reason for the low $(^{36}Ar/^{20}Ne)_{tr}$ ratios.

If the noble gas signature of a chondrule sample is dominated by contaminating matrix or surrounding MS, the measured $(^{36}Ar/^{20}Ne)_{tr}$ ratio would be matrix/MS-like. This is the case for 5 data points in Fig. 4, the $(^{36}Ar/^{20}Ne)_{tr}$ ratios of which are within uncertainties identical to those of the respective matrix and MS data (data points in brackets; see also Table A1). For those samples, a significant contamination is probable. Thus, they are not considered any further. Adsorbed air is expected to have a distinctly higher $^{36}Ar/^{20}Ne$ ratio than the atmospheric value of 1.9 (Table 1) since Ar usually sticks better to a sample surface than Ne. However, the chondrules have $(^{36}Ar/^{20}Ne)_{tr}$ ratios in the range of or even distinctly lower than unfractionated air. Therefore, it can be excluded that fractionated air significantly influences the $(^{36}Ar/^{20}Ne)_{tr}$ ratios.

The most important argument against the low $(^{36}Ar/^{20}Ne)_{tr}$ ratios being artifacts is as follows: average bulk samples of Semarkona, Bishunpur, and Renazzo (Fig. 4) have slightly lower $(^{36}Ar/^{20}Ne)$tr ratios than the respective matrices. Apart from the chondrules, there is no major constituent that could account for the decrease of the bulk $(^{36}Ar/^{20}Ne)_{tr}$ ratios compared to the matrix. For example, a mixture by mass of roughly 80% chondrules and 20% matrix ($[^{36}Ar/^{20}Ne]_{tr}$ ratios of ~3 and ~14, respectively) explains the bulk $(^{36}Ar/^{20}Ne)_{tr}$ ratio of Semarkona (~11). This is in accordance with average chondrule and matrix proportions of ordinary chondrites (e.g., Brearley and Jones 1998). The fact that the low $(^{36}Ar/^{20}Ne)_{tr}$ ratios of the chondrules are indeed due to an indigenous trapped component justifies using the subscript "tr" for it. In the following, we try to specify this component.

Heating of matrix-like precursor material with a given initial $(^{36}Ar/^{20}Ne)_{tr}$ ratio would lead to a noble gas fractionation toward higher $(^{36}Ar/^{20}Ne)_{tr}$ ratios. First, studies on primitive meteorites of different metamorphic stages and heating experiments showed that the major Ne-carrier (presolar diamonds) degasses at slightly lower temperatures than the major Ar-carrier (phase Q) (Huss et al. 1996; Nakasyo et al. 2000). Second, diffusive losses would alter the $^{36}Ar/^{20}Ne$ ratios toward higher values, opposite to the observed trend, because Ne diffuses faster than Ar. Therefore, we conclude that the low $(^{36}Ar/^{20}Ne)_{tr}$ ratios of the chondrules cannot be explained solely by heating of a matrix-like chondrule precursor. In fact, they indicate the presence of HL noble gases with a $^{36}Ar/^{20}Ne$ ratio of ~0.1, or SW noble gases with a $^{36}Ar/^{20}Ne$ ratio of ~0.04 (Table 1). Both components could be slightly mass fractionated or mixed with tiny amounts of matrix-like noble gases.

In summary, 15 of the chondrule samples measured for Ne contained small amounts of $^{20}Ne_{tr}$, and in 43 of the 47 samples measured for Ar, $^{36}Ar_{tr}$ could be detected. This is in contrast to more intensely melted calcium-aluminium-rich inclusions (CAIs; see Vogel 2003), which obviously lost all trapped Ne and Ar that might have been present in their precursor material. For 13 of the chondrule samples, $(^{36}Ar/^{20}Ne)_{tr}$ ratios could be given, of which 5 indicated matrix/MS contamination. The remaining samples show unusually low $(^{36}Ar/^{20}Ne)_{tr}$ ratios that cannot be explained as artifacts but indicate the presence of a HL or SW component.

RESULTS: METAL-SULFIDE-RICH SAMPLES

Ne and Ar Isotopic Composition of MS-Rich Samples and Correction for the Cosmogenic Component

We separated 14 MS-rich samples from Semarkona, Bishunpur, Krymka, and Renazzo. No such samples were available from our specimens of Allende and Leoville. The measured ^{20}Ne and ^{36}Ar concentrations and isotopic compositions of the MS-rich samples are given in Table A2. They generally have Ne isotopic compositions similar to those of the matrix samples of the respective meteorites

(compare Vogel et al. 2003). However, a regression of all MS-rich samples in a plot of $^{20}Ne/^{22}Ne$ versus $^{21}Ne/^{22}Ne$ (not shown) leads to a trapped $^{20}Ne/^{22}Ne$ ratio of ~9.6, i.e., slightly shifted to the composition of Ne-Q ($^{20}Ne/^{22}Ne$: 10.1–10.7; Busemannet al. 2000) compared to the generally HL-like ($^{20}Ne/^{22}Ne$: ~8.5; Huss and Lewis 1994a) trapped Ne isotopic composition of the bulk meteorites (e.g., Vogel et al. 2003).

Except for Renazzo, the $^{36}Ar/^{38}Ar$ ratios of the MS-rich samples indicate Q composition.

The cosmogenic correction of the measured ^{20}Ne and ^{36}Ar of the MS-rich samples was less delicate than that of the chondrules due to generally higher trapped noble gas concentrations. The correction was performed as described by Vogel et al. (2003) for matrix samples of the respective meteorites. This is justified because the $^{20}Ne/^{21}Ne$ ratio of cosmogenic Ne produced from iron and silicates is very similar: iron meteorites from different classes with exposure ages >>100 Ma, and, thus, essentially pure cosmogenic noble gas signatures, show a mean cosmogenic $^{20}Ne/^{21}Ne$ ratio of ~0.93 (Lavielle et al. 1999), i.e., identical to typical chondritic values. The variability of the $^{20}Ne/^{21}Ne$ ratios given by Lavielle and coworkers is small (standard deviation ~1%), indicating that variable S contents in the different iron meteorites do not significantly affect their $(^{20}Ne/^{21}Ne)_{cos}$ ratios. Also, the cosmogenic $^{36}Ar/^{38}Ar$ ratios of iron meteorites and chondritic material are basically identical (Wieler 2002).

Except for Renazzo, the resulting $^{20}Ne_{tr}$ and $^{36}Ar_{tr}$ concentrations (Table A2) of the MS-rich samples generally are in the range defined by the matrices (Fig. 5) precluding an air or blank origin of these noble gases. One MS-rich coating of Krymka (K-MSC-E) did not contain detectable amounts of $^{20}Ne_{tr}$. All Renazzo MS-samples show low $^{20}Ne_{tr}$ and $^{36}Ar_{tr}$ concentrations in the range of chondrule data.

$(^{36}Ar/^{20}Ne)_{tr}$ Ratios of Metal-Sulfide-Rich Samples

Figure 6 shows $(^{36}Ar/^{20}Ne)_{tr}$ ratios versus $^{36}Ar_{tr}$ concentrations of the MS-rich samples. Again, the respective matrix data are plotted for comparison. Although the MS-rich samples of Semarkona, Bishunpur, and Krymka roughly plot within the range defined by their respective matrix samples,

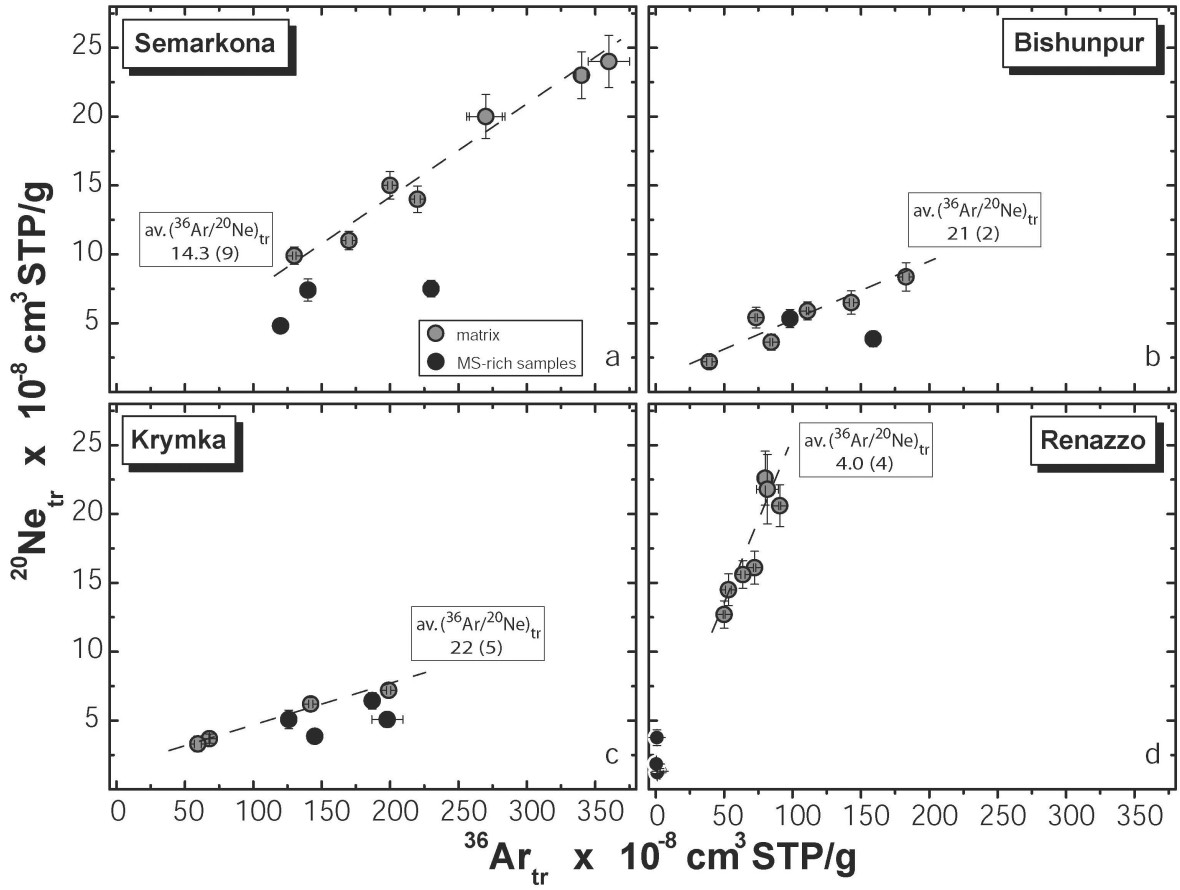

Fig. 5. Matrix (gray symbols) and metal-sulfide-rich samples (black symbols) of Semarkona, Bishunpur, Krymka, and Renazzo in plots of $^{20}Ne_{tr}$ versus $^{36}Ar_{tr}$. The numbers in boxes are average $(^{36}Ar/^{20}Ne)_{tr}$ ratios of the shown matrix samples. Many metal-sulfide-rich samples show noble gas concentrations comparable to those of the respective matrices and are partly enriched in ^{36}Ar relative to ^{20}Ne compared to the matrix. Renazzo metal-sulfide-rich samples have $^{20}Ne_{tr}$ and $^{36}Ar_{tr}$ concentrations in the range of chondrule values. Error bars are 1σ.

some of them display a general trend of increasing ($^{36}Ar/^{20}Ne)_{tr}$ ratios with increasing $^{36}Ar_{tr}$ concentrations (grey arrows in Figs. 6a–6c) compared to the respective matrix samples. This may indicate mixing of a hypothetical "MS end member" with a high $(^{36}Ar/^{20}Ne)_{tr}$ ratio and $^{36}Ar_{tr}$ concentration and a matrix end member that is lower in $(^{36}Ar/^{20}Ne)_{tr}$ and $^{36}Ar_{tr}$.

The 2 Bishunpur MS-rich coatings (B-MSC-A, B-MSC-F; Fig. 1d) have different noble gas signatures. While B-MSC-A shows a high $(^{36}Ar/^{20}Ne)_{tr}$ ratio and $^{36}Ar_{tr}$ concentration, B-MSC-F plots in the range of Bishunpur matrix (Fig. 6b). This difference is probably related to different textures of the 2 MS-rich samples and allows us to draw conclusions about the noble gas signatures in MS-rich coatings in general (see below). The noble gas signatures of Renazzo MS-rich samples differ significantly from those of Semarkona, Bishunpur, and Krymka. All Renazzo MS-rich samples have distinctly lower $(^{36}Ar/^{20}Ne)_{tr}$ ratios and $^{36}Ar_{tr}$ concentrations than Renazzo matrix and plot in the range of chondrule data (Figs. 4 and 6d).

DISCUSSION

We found small but measurable amounts of trapped ^{20}Ne in some and trapped ^{36}Ar in many of the studied chondrules of the primitive CV, CR, and LL chondrites. Those chondrules containing both indigeneous $^{20}Ne_{tr}$ and $^{36}Ar_{tr}$ show low $(^{36}Ar/^{20}Ne)_{tr}$ ratios compared to the surrounding matrix. This could point to the presence of small amounts of either presolar diamond noble gases of HL composition or SW noble gases. Below, we discuss the origin of the chondrule noble gases taking into account the noble gas signatures of the genetically related MS-rich samples.

Solar or Presolar Diamond-Like Noble Gases in Chondrules?

Unfractionated or fractionated solar noble gases in chondrules of otherwise solar gas-free meteorites would support an exposure of the chondrules or their precursor material, respectively, to solar radiation before their

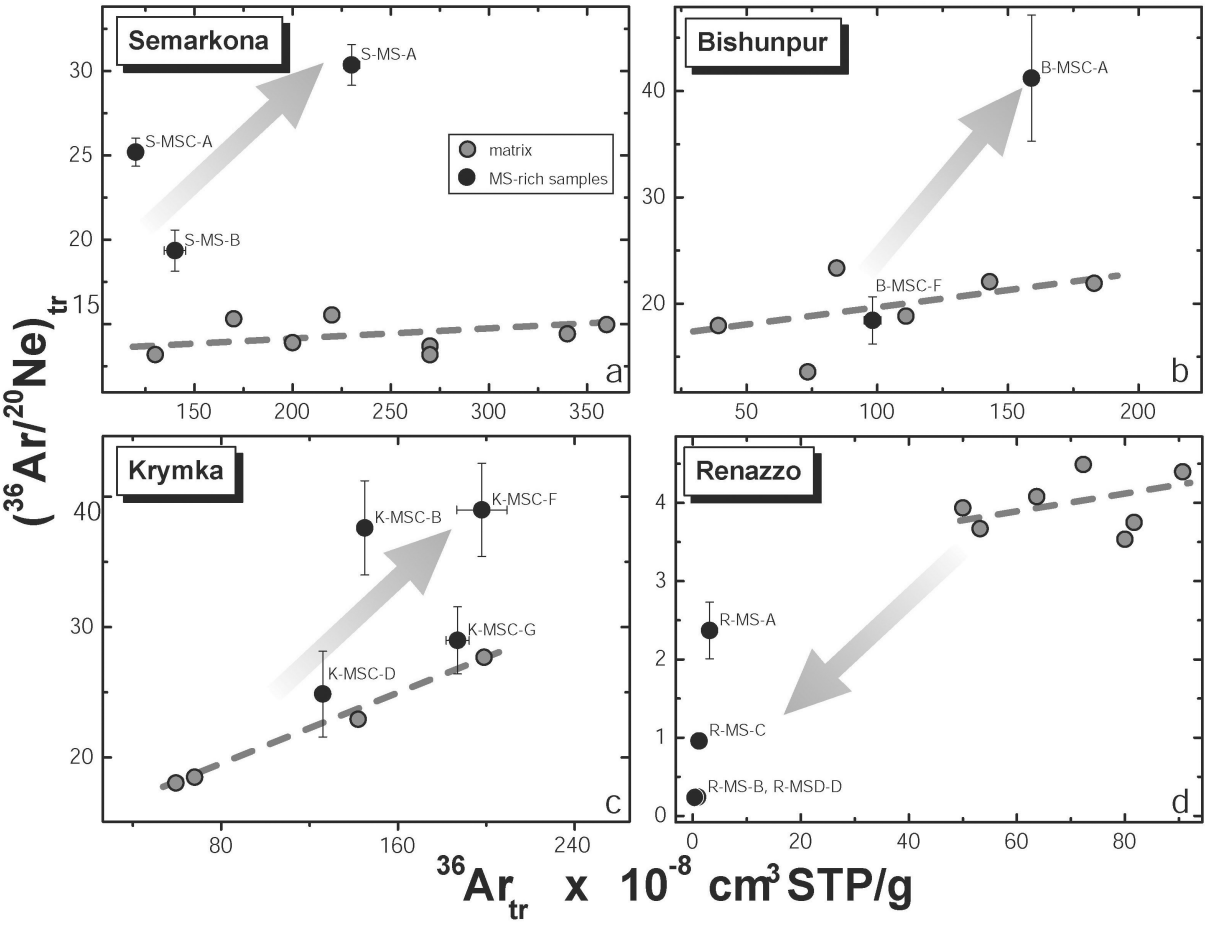

Fig. 6. $(^{36}Ar/^{20}Ne)_{tr}$ ratios versus ^{36}Ar concentrations of the metal-sulfide-rich samples of Semarkona, Bishunpur, Krymka, and Renazzo (black symbols). Compared to the respective matrices (gray symbols), many of the metal-sulfide-rich samples are enriched in $^{36}Ar_{tr}$ relative to the $^{20}Ne_{tr}$, resulting in the upward trends marked with gray arrows. Only the 4 metal-sulfide-rich samples of Renazzo have low $(^{36}Ar/^{20}Ne)_{tr}$ ratios and ^{36}Ar concentrations similar to chondrules. Error bars are 1σ.

incorporation into a parent body. Strong SW irradiation of the chondrule precursor material was assumed by Okazaki et al. (2001b) to explain the high amounts of "subsolar" (i.e., strongly mass fractionated compared to SW) noble gases in chondrules of the enstatite chondrite Y-791790. Apart from the possibility that this interpretation might have to be reassessed if it should be confirmed that not only the enstatite chondrite St. Mark's studied by Busemann et al. (2003) but "subsolar" gas-bearing meteorites in general contain a fraction of unaltered solar elemental composition, we think that our chondrule data cannot be explained the same way as those of Okazaki et al. (2001b). Our chondrules contain much lower trapped noble gas concentrations and $(^{36}Ar/^{20}Ne)_{tr}$ ratios very different from a "subsolar" composition but similar to rather unfractionated SW noble gases. The latter would imply a weak SW irradiation after the chondrules had been created but before they were incorporated into a parent body. Such a scenario is not supported by the ^{4}He concentrations in our chondrules in the range of $1–3 \times 10^{-5}$ cm^3STP/g. These are typical concentrations expected from radioactive decay of U and Th and, hence, leave hardly any room for additions of solar ^{4}He (assuming a roughly unfractionated solar $^{4}He/^{20}Ne$ of ~600; Wieler 2002). Therefore, we consider the presence of solar noble gases in the studied chondrules as very unlikely and explain the noble gas signature of the chondrules by the presence of small amounts of HL noble gases from presolar diamonds.

Assuming a matrix-like chondrule precursor material, a "pure" HL-like signature in the chondrules requires a preferential removal during chondrule formation of phase Q and its noble gases. Simple heating of a matrix-like precursor would produce a high $(^{36}Ar/^{20}Ne)_{tr}$ ratio of the chondrules, which is in contrast to what we observe. Therefore, a mechanism that removes the ^{36}Ar-carrying phase Q from the chondrules is necessary to explain their low, HL-like $(^{36}Ar/^{20}Ne)_{tr}$ ratios. Such a mechanism could be the metal-silicate separation that occurred during chondrule formation: metal-sulfides are often associated with carbonaceous material that entered the metal phase during chondrule formation (Kong and Ebihara 1997; Kong et al. 1999; Mostefaoui and Perron 1994). Since phase Q is carbonaceous as well (e.g., Ott et al. 1981), it is possible that it also got associated to the metal phase during melting. This could simultaneously explain the depletion of $^{36}Ar_{tr}$ relative to $^{20}Ne_{tr}$ in the chondrules and the $^{36}Ar_{tr}$ enrichment in surrounding MS-rich coatings compared to the matrix of the respective meteorites.

In the next section, we present a literature overview about the formation of MS and the role of carbonaceous material during chondrule formation, including cases where a relationship between meteoritic metal, carbonaceous material, and $^{36}Ar_{tr}$ seems to exist. Based on this background, we finally discuss our model, in which the HL and Q carrier phases are fractionated by metal-silicate separation during chondrule formation.

The Origin of Metal-Sulfides and the Role of Carbon During Chondrule Formation

The relationship between MS and chondrules in enstatite, ordinary, and CR chondrites has been extensively studied (Connolly et al. 2001; Grossman and Wasson 1985, 1987; Kong and Palme 1999; Kong and Ebihara 1996, 1997; Kong et al. 1999; Mostefaoui and Perron 1994; Rambaldi and Wasson 1981, 1984; Zanda et al. 1994). It is generally argued that MS was either created during chondrule formation by the reduction of a matrix-like precursor (Alexander 1989; Connolly et al. 2001; Kong and Ebihara 1996; Kong and Palme 1999) or that it had been present already in the precursor (Grossman and Wasson 1985; Kong and Palme 1999; Zanda et al. 2002). In both scenarios, liquid metal droplets were separated from the silicate melt during chondrule formation. The droplets eventually migrated to the chondrule margins (Connolly et al. 2001; Grossman and Wasson 1987; Humayun et al. 2002; Kong and Palme 1999; Kong et al. 1999) where some of them solidified while being expelled from chondrules and formed compact MS-rich coatings ("expelled" coatings) (e.g., Alexander 1989). Others were completely separated from their host chondrules and may be found as isolated blebs within chondrite matrices (Connolly et al. 2001; Humayun et al. 2002; Mostefaoui and Perron 1994). In other cases, MS evaporated from molten chondrules and recondensed onto chondrule surfaces ("recondensed" coatings) (Alexander 1989; Connolly et al. 2001; Kong and Palme 1999). Kojima et al. (2003) discuss the final extraction of MS from Bishunpur chondrules and the formation of coatings during impacts on parent bodies.

Metallic phases in unequilibrated chondrites are often associated with carbonaceous material (e.g., Kong and Ebihara 1997; Kong et al. 1999; Mostefaoui and Perron 1994, and references therein). During chondrule melting, organic material was possibly decomposed, dissolved into the metal, and later released to form thin layers around metal grains (e.g., Kong et al. 1999, and references therein). Carbonaceous material in the chondrule precursor possibly also played a major role in the formation of metal during chondrule melting. Connolly et al. (2001) estimated that 2–4 wt% of C, which is in the range of carbon concentrations in CM and CI chondrite matrices, are needed to reduce precursor FeO and NiO. Excess carbon forms graphite grains associated with the metal (Connolly et al. 1994).

Swindle et al. (1991) found that small amounts of heavy trapped noble gases in chondrules from the LL3 chondrite Chainpur were associated with the siderophile-chalcophile component of the chondrules, including, e.g., Fe, Ni, and sulfides. The authors attributed this to an affinity of carbon to the metal phase and suggested that noble gases were retained during chondrule formation. Also, in some differentiated meteorites, a relationship between metal, carbonaceous material, and ^{36}Ar concentration exists. The IAB iron meteorite Bohumilitz has graphite inclusions containing ^{36}Ar-Q in its

metallic matrix (Maruoka et al. 2001). In the achondrite Lodran, high ^{36}Ar concentrations of up to 85×10^{-8} cm^{3}STP/g were found in Fe-Ni-separates (Busemann and Eugster 2000; Weigel 1996). Retrapping of the noble gases in bubbles (Busemann and Eugster 2000), or graphite inclusions as possible carrier phases of the noble gases (Weigel 1996), have been discussed.

In summary, the formation of metallic phases is probably related to chondrule formation, and metallic phases are often associated with carbonaceous material. Metal, carbonaceous material, and ^{36}Ar-Q are reported to be correlated in chondrules of Chainpur and in some differentiated meteorites. Since the ^{36}Ar carrier phase Q is also carbonaceous, our preferred explanation of the enrichment of ^{36}Ar in some of our MS-rich samples is by the association of metal and carbonaceous material.

Fractionation of Phase Q and Presolar Diamond Noble Gases During Chondrule Formation?

Chondrules most probably formed from primitive matrix-like precursor material hosting the major carriers for primordial noble gases, phase Q and presolar diamonds. Based on the correlation of siderophile elements and heavy trapped noble gases in chondrules of Chainpur (Swindle et al. 1991) and the observation that Q gases also occur correlated with carbonaceous material in the metal phases of differentiated meteorites, we expect a siderophile behavior of phase Q during chondrule formation. From the above results, we further infer that the presolar diamonds—although also being carbonaceous—display less affinity to MS than phase Q. This would imply a partial separability of phase Q and presolar diamonds, which is in agreement with results of Matsuda et al. (1999) who succeeded in separating the two carrier phases to a certain degree.

Assuming that the MS coatings were formed during chondrule formation, we propose that the studied chondrules were created in transient flash-heating events in a dust-rich environment (see, e.g., Scott et al. 1996). During melting of the matrix-like precursor material, the Q carrier entered the MS more efficiently than the presolar diamonds. The MS migrated outward and solidified quickly at chondrule margins. Probably, phase Q (and its Ar-rich noble gas inventory) survived this short high temperature event encapsulated in the metal phase. In principle, it is also possible that the noble gases were released and immediately retrapped in the solidifying MS. Eutectic melting of chondritic Fe, Ni-FeS already starts at 950 °C (Benedix et al. 2000). The liquidus temperatures experienced by chondrules are in the range of 1350 to 1800 °C (Cohen et al. 2000, and references therein). These temperatures are below the maximum release temperatures of noble gases of phase Q (1100–≥1800 °C; Huss et al. 1996) thus, phase Q could—at least for a short time—partly survive in a molten metallic phase. Simultaneously, fine-grained matrix-like dust was admixed to the molten MS coatings and added variable amounts of noble gases with a matrix-like signature. The final noble gas signature of the expelled MS-rich coatings, therefore, is a mixture of the ^{36}Ar-(Q)-rich MS and the matrix-like noble gas signature of the accreted dust. Thus, the MS-rich samples eventually have higher $(^{36}Ar/^{20}Ne)_{tr}$ ratios than the respective pure matrix-like material, and also, their Ne isotopic signatures indicate an enrichment in phase Q. While phase Q was extracted from the chondrules, the ^{20}Ne-carrying presolar diamonds remained preferentially—relative to phase Q—in the molten chondrule interior. Thereby, most of the diamonds broke down and released their noble gases. In fact, the diamonds have a relatively large range of release temperatures roughly between 1100–1600 °C, pointing to variably stable subgroups (Huss and Lewis 1994a, b). We suggest that only the most resistant presolar diamonds survived the chondrule heating event. Similar noble gas signatures in chondrules and the MS coatings would be expected in the scenario proposed by Kojima et al. (2003) where the final MS extraction from chondrules was induced by impacts on parent bodies.

Finally, the noble gas signatures of the MS coatings might have been aquired—independently from the chondrules—by equilibration of the MS with the nebular gas and addition of matrix-like dust. However, our data argue against this scenario. First, the inferred trapped ^{20}Ne/^{22}Ne ratio of the MS of ~9.6 indicates a mixture of noble gases of HL and Q composition rather than a nebular, i.e., solar signature with a ^{20}Ne/^{22}Ne ratio of ~13.7 (Wieler 2002). Also, the $(^{36}Ar/^{20}Ne)_{tr}$ ratios of the MS (see Table A2) are very different from nebular ^{36}Ar/^{20}Ne ratios in the range of ~0.04. Further, the nebular Ne and Ar pressures required to explain the trapped Ne and Ar concentrations in the MS as a result of dissolution of nebular noble gases into the studied MS would be several orders of magnitude higher than the actual Ne and Ar partial pressures in the nebula (e.g., Pepin 1991), even if one takes into account that a part of the MS noble gases originates from admixed matrix. For the estimate, experimentally determined solubilities for Ne and Ar in an enstatite melt (Kirsten 1968) were used. Adsorption of Ne and Ar to the MS is further improbable, since this would require low temperatures during or right after chondrule formation and would also have brought substantial amounts of water to the coated chondrules, which is not observed. Also, the 2 Bishunpur MS-rich coatings argue against this scenario. B-MSC-A is a thick compact coating typical for expelled MS (e.g., Alexander 1989). It clearly shows an enhanced $(^{36}Ar/^{20}Ne)_{tr}$ ratio relative to the matrix. In contrast, B-MSC-F is a recondensed coating with a layered texture, and it is separated from the chondrule by a thin fine-grained clastic rim (not visible in Fig. 1d). This MS-rich coating does not show a $^{36}Ar_{tr}$-enrichment but a $(^{36}Ar/^{20}Ne)_{tr}$ ratio identical to the surrounding matrix. In this case, the MS evaporated from the chondrule margins, thereby releasing the entrapped Q gases.

During recondensation back onto a chondrule, substantial amounts of noble gas-rich matrix-like dust accreted simultaneously, which exclusively determined the final noble gas signature of the recondensed MS-rich coating. If the enhancement of the $(^{36}Ar/^{20}Ne)_{tr}$ ratio in the MS-rich coating compared to its respective matrix would have been caused by reactions of MS with the nebular gas, we would expect a higher $(^{36}Ar/^{20}Ne)_{tr}$ in the recondensed Bishunpur coating than in the expelled one, which contradicts our results. Therefore, we conclude that the noble gas signatures of the MS-rich coatings, generally, were not determined by the ambient nebular gas.

The MS droplet from the interior of a Renazzo chondrule (R-MSD-B) has the same unusually low $(^{36}Ar/^{20}Ne)_{tr}$ ratio as the MS-rich coating and the MS droplets associated with Renazzo matrix. This also proves the genetic relationship between these different occurences of MS and further rules out the possibility that the noble gas signatures of MS coatings and matrix MS were controlled by the ambient nebular gas. However, it is difficult to straightforwardly explain the low $(^{36}Ar/^{20}Ne)_{tr}$ ratios of these MS samples, which are in the range of chondrule values. Possibly, the chondrule precursor had already been more highly depleted in Q than in HL gases. A hint for this might come, e.g., from the low $(^{36}Ar/^{20}Ne)_{tr}$ ratios of the Renazzo matrix. A chondrule precursor already depleted in volatiles is also proposed by Humayun et al. (2002) to explain the net depletion of volatiles in Renazzo.

Implications for Chondrule Formation Scenarios

As summarized above, chondrules and their associated MS-rich coatings are often genetically related. This is supported by our noble gas data showing complementary noble gas signatures of chondrules and most of the studied MS-rich samples. If the MS coatings were formed simultaneously with the chondrules themselves, the presence of fine-grained matrix-like material intimately mixed with the MS-rich samples in their molten stage points to a formation of the chondrules and their MS-rich coatings during transient high temperature events in a dust-rich environment. The general similarity of the trapped Ne and Ar concentrations and $^{36}Ar/^{20}Ne$ ratios of the matrix-like material and the MS-rich samples of Semarkona, Bishunpur, and Krymka further supports a fairly quick "local" accretion of all constituents to their ordinary chondrite parent body. Otherwise, the chondrules with their MS-rich coatings might have been separated from the respective enveloping dust volumes and might have accreted in different nebular areas with distinctly different noble gas signatures. Such a local accretion is in accordance with the results by Klerner (2001) and Kong and Palme (1999), who postulate a close relationship between chondrules and matrix in carbonaceous chondrites on the basis of main and trace element distributions between both constituents. However, our data would also be consistent with an extraction of the MS from chondrules during a later impact event on a parent body (Kojima et al. 2003).

Due to very different concentrations and elemental ratios of trapped noble gases, our chondrule data cannot be explained as proposed by Okazaki et al. (2001b) for the chondrules of the enstatite chondrite Y-791790. If the data for the chondrules of the enstatite chondrite are confirmed, the possibility would have to be considered that different chondrule populations might have been formed by basically different mechanisms.

CONCLUSIONS

We found low but discernible concentrations of trapped ^{20}Ne in some and trapped ^{36}Ar in most of the studied chondrules of the CV, CR, and LL chondrites Allende, Leoville, Renazzo, Semarkona, Bishunpur, and Krymka. We conclude that the melting event during which these chondrules were formed was not intense enough to fully release the noble gases present in the chondrule precursor. This is in contrast to CAIs that have lost all of the trapped Ne and Ar that might have been present in their precursor material (Vogel 2003), obviously because they experienced a prononged high temperature processing. For some chondrules, $(^{36}Ar/^{20}Ne)_{tr}$ ratios also could be determined. These were unexpectedly low compared to the $(^{36}Ar/^{20}Ne)_{tr}$ ratios of the respective matrices. We also measured samples of metal-sulfide-rich material occurring mainly as coatings around chondrules but also as isolated patches in the matrix and within chondrules. Except for Renazzo, these show $(^{36}Ar/^{20}Ne)_{tr}$ ratios in the range of, or slightly higher than, those of the matrix of the respective chondrites. Our preferred explanation is that the low $(^{36}Ar/^{20}Ne)_{tr}$ ratios of the chondrules were established by fractionation of the major trapped noble gas carriers, phase Q and presolar diamonds, during chondrule formation from a matrix-like precursor. The fractionation occurred during metal-silicate separation in the molten chondrules. This simultaneously explains the low $(^{36}Ar/^{20}Ne)_{tr}$ ratios in the chondrules and the higher $(^{36}Ar/^{20}Ne)_{tr}$ ratios of MS-rich coatings compared to surrounding matrix: the carbonaceous phase Q was preferentially enriched in the metallic phase that migrated to the chondrule margins and eventually coated them. Within the chondrules, only the most resistant presolar diamonds survived the heating, hence, the chondrules display a HL-like noble gas signature.

The admixture of matrix-like material to the molten MS-rich coatings supports chondrule formation by transient heating events in a dust-rich environment. The similarity of the Q-like noble gas signatures of the MS-rich coatings and the matrix of the studied ordinary chondrites then might point to a quick accretion of coated chondrules and fine-grained material to parent bodies without previous large-scale

chondrule transport, as it would be required in the framework of the X-wind model (Shu et al. 1997, 2001).

Our chondrule data are very different from those of an enstatite chondrite presented by Okazaki and coworkers (2001b). This suggests that the processes that created the chondrules studied by us and those of the enstatite chondrite Y-791790 probably were not the same. It is well imaginable that different chondrule formation mechanisms were active simultaneously in different regions of the solar system.

Acknowledgments–We thank the following institutions for providing sample material: the Muséum National d'Histoire Naturelle (Paris) for Renazzo, the Smithsonian National Museum of Natural History (Washington D.C.) for Semarkona, the Natural History Museum (London) for Bishunpur, and the SSC of Environmental Radiochemistry (Kyiv) for Krymka. We appreciate the constructive reviews provided by T. Nakamura and T. Swindle. Further, we would like to thank T. Grund, A. Baarnholm, and K. Kunze for competent assistance with SEM work. This work was supported by the Swiss National Science Foundation.

Editorial Handling—Dr. Marc Caffee

REFERENCES

Alexander C. M. O. 1989. Origin of chondrule rims and interchondrule matrices in unequilibrated ordinary chondrites. *Earth and Planetary Science Letters* 95:187–207.

Benedix G. K., McCoy T. J., Keil K., and Love S. G. 2000. A petrologic study of the IAB iron meteorites: Constraints on the formation of the IAB-winonaite parent body. *Meteoritics & Planetary Science* 35:1127–1141.

Benkert J. P., Baur H., Signer P., and Wieler R. 1993. He, Ne, and Ar from the solar wind and solar energetic particles in lunar ilmenites and pyroxenes. *Journal of Geophysical Research* 98: 13147–13162.

Brearley A. J. and Jones R. H. 1998. Chondritic meteorites. In *Planetary materials,* edited by Papike J. J. Washington D.C.: Mineralogical Society of America. pp. 3.1–3.398.

Busemann H. and Eugster O. 2000. Primordial noble gases in Lodran metal separates and the Tatahouine diogenite (abstract #1642). 31st Lunar and Planetary Science Conference.

Busemann H., Baur H., and Wieler R. 2000. Primordial noble gases in "phase Q" in carbonaceous and ordinary chondrites studied by closed-system stepped etching. *Meteoritics & Planetary Science* 35:949–973.

Busemann H., Baur H., and Wieler R. 2002. Phase Q—A carrier for subsolar noble gases (abstract #1462). 33rd Lunar and Planetary Science Conference.

Busemann H., Eugster O., Baur H., and Wieler R. 2003. The ingredients of the "subsolar" noble gas component (abstract #1774). 33rd Lunar and Planetary Science Conference.

Cohen B. A., Hewins R. H., and Yu Y. 2000. Evaporation in the young solar nebula as the origin of "just-right" melting of chondrules. *Nature* 406:600–602.

Connolly H. C., Hewins R. H., Ash R. D., Zanda B., Lofgren G. E., and Bourot-Denise M. 1994. Carbon and the formation of reduced chondrules. *Nature* 371:136–139.

Connolly H. C., Huss G. R., and Wasserburg G. J. 2001. On the formation of Fe-Ni metal in Renazzo-like carbonaceous chondrites. *Geochimica et Cosmochimica Acta* 65:4567–4588.

Crabb J. and Anders E. 1981. Noble gases in E chondrites. *Geochimica et Cosmochimica Acta* 45:2443–2464.

Eberhardt P., Eugster O., and Marti K. 1965. A redetermination of the isotopic composition of atmospheric neon. *Zeitschrift für Naturforschung* 20a:623–624.

Eugster O. 1988. Cosmic ray production rates for ^{3}He, ^{21}Ne, ^{38}Ar, and ^{126}Xe in chondrites based on ^{81}Kr-Kr exposure ages. *Geochimica et Cosmochimica Acta* 52:1649–1662.

Grossman N. J. and Wasson J. T. 1985. The origin and history of the metal and sulfide components of chondrules. *Geochimica et Cosmochimica Acta* 49:925–939.

Grossman N. J. and Wasson J. T. 1987. Compositional evidence regarding the origin of rims on Semarkona chondrules. *Geochimica et Cosmochimica Acta* 51:3003–3011.

Grossmann N. J., Rubin A. E., Nagahara H., King E. A. 1988. Properties of chondrules. In *Meteorites and the early solar system,* edited by Kerridge J. F. and Matthews M. S. Tucson: The University of Arizona Press. pp 619–659.

Huang S., Lu J., Prinz M., Weisberg M. K., Benoit H. P., and Sears D. W. G. 1996. Chondrules: Their diversity and the role of open-system processes during their formation. *Icarus* 122:316–346.

Humayun M., Campbell A. J., Zanda B., and Bourot-Denise M. 2002. Formation of Renazzo chondrule metal inferred from siderophile elements (abstract #1965). 32nd Lunar and Planetary Science Conference.

Huss G. R. and Lewis R. S. 1994a. Noble gases in presolar diamonds I: Three distinct components and their implications for diamond origins. *Meteoritics* 29:791–810.

Huss G. S. and Lewis R. S. 1994b. Noble gases in presolar diamonds II: Component abundances reflect thermal processing. *Meteoritics* 29:811–829.

Huss G. R., Lewis R. S., and Hemkin S. 1996. The "normal planetary" noble gas component in primitive chondrites: Compositions, carrier, and metamorphic history. *Geochimica et Cosmochimica Acta* 60:3311–3340.

Kim J. S. and Marti K. 1994. Distribution of some highly volatile elements in chondrules (abstract). *Meteoritics* 29:482.

Kirsten T. 1968. Incorporation of rare gases in solidifying enstatite melts. *Journal of Geophysical Research* 73:2807–2810.

Klerner S. 2001. Materie im frühen Sonnensystem: Die Entstehung von Chondren, Matrix und refraktären Forsteriten. Ph.D. thesis, Universität zu Köln, Köln, Germany.

Kojima T., Lauretta D. S., and Buseck P. R. 2003. Accretion, dispersal, and reaccumulation of the Bishunpur (LL3.1) brecciated chondrite. Evidence from troilite-silicate-metal inclusions and chondrule rims. *Geochimica et Cosmochimica Acta* 67:3065–3078.

Kong P. and Ebihara M. 1996. Metal phases of L chondrites: Their formation and evolution in the nebula and in the parent body. *Geochimica et Cosmochimica Acta* 60:2667–2680.

Kong P. and Ebihara M. 1997. The origin and nebular history of the metal phase of ordinary chondrites. *Geochimica et Cosmochimica Acta* 61:2317–2329.

Kong P. and Palme H. 1999. Compositional and genetic relationship between chondrules, chondrule rims, metal, and matrix in the Renazzo chondrite. *Geochimica et Cosmochimica Acta* 63:3673–3682.

Kong P., Ebihara M., and Palme H. 1999. Distribution of siderophile elements in CR chondrites: Evidence for evaporation and recondensation during chondrule formation. *Geochimica et Cosmochimica Acta* 63:2637–2652.

Lavielle B., Marti K., Jeannot J.-P., Nishiizumi K., and Caffee M. 1999. The ^{36}Cl-^{36}Ar-^{40}K-^{41}K records and cosmic ray production

rates in iron meteorites. *Earth and Planetary Science Letters* 170: 93–104.
Lewis R. S., Srinivasan B., and Anders E. 1975. Host phase of a strange xenon component in Allende. *Science* 190:1251–1262.
Leya I., Lange H. J., Neumann S., Wieler R., and Michel R. 2000. The production of cosmogenic nuclides in stony meteoroids by galactic cosmic-ray particles. *Meteoritics & Planetary Science* 35:259–286.
Maruoka T., Matsuda J., and Kurat G. 2001. Abundance and isotopic composition of noble gases in metal and graphite of the Bohumilitz IAB iron meteorite. *Meteoritics & Planetary Science* 36:597–609.
Mason B. 1979. Cosmochemistry Part 1. Meteorites. In *Data of geochemistry,* edited by Fleischer F. Geological Survey Professional Paper 440-B-1. Washington D.C.: U.S. Government Printing Office. pp B1–B132.
Matsuda J., Amari S., and Nagao K. 1999. Purely physical separation of a small fraction of the Allende meteorite that is highly enriched in noble gases. *Meteoritics & Planetary Science* 34: 129–136.
McSween H. Y., Fronabarger K., and Driese S. G. 1983. Ferromagnesian chondrules in carbonaceous chondrites. In *Chondrules and their origins,* edited by King E. A. Houston: Lunar and Planetary Institute. pp. 195–210.
Miura Y. N. and Nagao K. 1996. Noble gases in chondrules of the Allende CV3 chondrite (abstract). *Meteoritics & Planetary Science* 31:A91.
Mostefaoui S. and Perron C. 1994. Carbon in the metal of Bishunpur and other ordinary chondrites (abstract). 25th Lunar and Planetary Science Conference. pp. 945–946.
Nakamura T., Nagao K., and Takaoka N. 1999. Microdistribution of primordial noble gases in CM chondrites determined by in situ laser microprobe analysis: Decipherment of nebular processes. *Geochimica et Cosmochimica Acta* 63:241–255.
Nakasyo E., Maruoka T., Matsumoto T., and Matsuda J. 2000. A laboratory experiment on the influence of aqueous alteration on noble gas composition in the Allende meteorite. *Antarctic Meteorite Research* 13:135–144.
Nier A. O. 1950. A redetermination of the relative abundances of the isotopes of carbon, nitrogen, oxygen, argon, and potassium. *Physical Review* 77:789–793.
Okazaki R., Nagao K., Takaoka N., and Nakamura T. 2001a. Studies of trapped noble gases in enstatite chondrites by laser microprobe techniques (abstract). *Meteoritics & Planetary Science* 36: A152–A153.
Okazaki R., Takaoka N., Nagao K., Sekiya M., and Nakamura T. 2001b. Noble-gas-rich chondrules in an enstatite meteorite. *Nature* 412:795–798.
Ott U. 2002. Noble gases in meteorites—Trapped components. In *Noble gases in geochemistry and cosmochemistry,* edited by Porcelli D., Ballentine C. J., and Wieler R. Washington D.C.: Mineralogical Society of America. pp. 71–100.
Ott U., Mack R., and Chang S. 1981. Noble-gas-rich separates from the Allende meteorite. *Geochimica et Cosmochimica Acta* 45: 1751–1788.
Ozima M. and Podosek F. A. 2002. *Noble gas geochemistry.* Cambridge: Cambridge University Press. 286 p.
Patzer A. and Schultz L. 2002. Noble gases in enstatite chondrites II: The trapped component. *Meteoritics & Planetary Science* 37: 601–612.
Pepin R. O. 1991. On the origin and early evolution of terrestrial planet atmospheres and meteoritic volatiles. *Icarus* 92:2–79.
Rambaldi E. R. and Wasson J. T. 1981. Metal and associated phases in Bishunpur, a highly unequilibrated ordinary chondrite. *Geochimica et Cosmochimica Acta* 45:1001–1015.
Rambaldi E. R. and Wasson J. T. 1984. Metal and associated phases in Krymka and Chainpur: Nebular formational processes. *Geochimica et Cosmochimica Acta* 48:1885–1897.
Rubin A. E. 2000. Petrologic, geochemical, and experimental constraints on models of chondrule formation. *Earth Science Reviews* 50:3–27.
Schultz L. and Franke L. 2000. Helium, neon, and argon in meteorites. A data collection. Update 2000. MPI-Chemie, Mainz, Germany.
Scott E. R. D. and Taylor G. J. 1983. Chondrules and other components in C, O, and E chondrites: Similarities in their properties and origins. Proceedings, 14th Lunar and Planetary Science Conference. *Journal of Geophysical Research* 88:B275–B286.
Scott E. R. D., Love S. G., and Krot A. N. 1996. Formation of chondrules and chondrites in the proto-planetary nebula. In *Chondrules and the protoplanetary disk,* edited by Hewins R. H., Jones R. H., and Scott E.R.D. Cambridge: Cambridge University Press. pp. 87–96.
Semenenko V. P., Bischoff A., Weber I., Perron C., and Girich A. L. 2001. Mineralogy of fine-grained material in the Krymka (LL3.1) chondrite. *Meteoritics & Planetary Science* 36:1067–1086.
Shu F. H., Shang H., Glassgold A. E., and Lee T. 1997. X-rays and fluctuating X-winds from proto-stars. *Science* 277:1475–1479.
Shu F. H., Shang H., Gounelle M., Glassgold A. E., and Lee T. 2001. The origin of chondrules and refractory inclusions in chondritic meteorites. *The Astrophysical Journal* 548:1029–1050.
Smith P. S., Huneke J. C., Rajan R. S., and Wasserburg G. J. 1977. Neon and argon in the Allende meteorite. *Geochimica et Cosmochimica Acta* 41:627–647.
Swindle T. D., Caffee M., Hohenberg C. M., Lindstrom M. M., and Taylor G. J. 1991. Iodine-xenon studies of petrographically and chemically characterized Chainpur chondrules. *Geochimica et Cosmochimica Acta* 55:861–880.
Vogel N. 2003. Chondrule formation and accretion processes in the early solar nebula—Clues from noble gases in different constituents of unequilibrated chondrites. Ph.D. thesis, ETH Zürich, Zürich, Switzerland.
Vogel N., Wieler R., Bischoff A., and Baur H. 2003. Microdistribution of primordial Ne and Ar in fine-grained rims, matrices, and dark inclusions of unequilibrated chondrites—Clues on nebular processes. *Meteoritics & Planetary Science* 38: 1399–1416.
Weigel A. S. 1996. Untersuchung der Entstehungsgeschichte von Achondriten anhand von Edelgas-Isotopenanalysen sowie Entwicklung eines Extraktions-, Reinigungs-, und Analysesystems für Stickstoff. Ph.D. thesis, Universität Bern, Bern, Switzerland.
Wieler R. 2002. Cosmic ray-produced noble gases in meteorites. In *Noble gases in geochemistry and cosmochemistry,* edited by Porcelli D., Ballentine C. J., and Wieler R. Washington D.C.: Mineralogical Society of America. pp. 125–170.
Zanda B., Bourot-Denise M., and Hewins R. H. 1994. Origin and metamorphic redistribution of silicon, chromium, and phosphorus in the metal of chondrites. *Science* 265:1846–1849.
Zanda B., Bourot-Denise M., Perron C., and Hewins R. H. 2002. Accretion textures, iron evaporation and re-condensation in Renazzo (abstract #1852). 33rd Lunar and Planetary Science Conference.

APPENDIX

Table A1. Ne and Ar isotopic and elemental compositions, $^{20}Ne_{tr}$, $^{36}Ar_{tr}$ concentrations, and $(^{36}Ar/^{20}Ne)_{tr}$ ratios of Allende, Leoville, Renazzo, Semarkona, Bishunpur, and Krymka chondrules. Also given are blank contributions to $^{20}Ne_{tr}$ and $^{36}Ar_{tr}$ concentrations (%).[a]

Sample[b]	Weight (g) ×10^{-4}	^{20}Ne	$^{20}Ne/^{22}Ne$	$^{21}Ne/^{22}Ne$	^{36}Ar	$^{36}Ar/^{38}Ar$	$^{20}Ne_{tr}$	$^{36}Ar_{tr}$	$(^{36}Ar/^{20}Ne)_{tr}$[c]	Blank contr. to $^{20}Ne_{tr}$	Blank contr. to $^{36}Ar_{tr}$
A-CH-A1	1.71(2)	3.33(8)	1.13(4)	0.89(3)	3.75(6)	4.45(8)	1.0(4)	3.6(4)	{4(1)}	10	4
A-CH-A2	0.20(1)	3.1(6)	1.0(2)	0.8(1)	1.2(3)	3(1)	*1(1)*	1.1(5)	–	91	62
A-CH-B	7.6(4)	3.9(2)	1.38(2)	0.85(2)	4.2(2)	4.45(5)	1.7(5)	4.1(5)	{2.4(7)}	1	1
A-CH-C1	2.35(2)	2.85(9)	0.97(3)	0.97(2)	1.18(2)	2.64(6)	0.5(3)	1.0(1)	{2(1)}	12	6
A-CH-C2	0.939(9)	3.0(1)	0.89(5)	0.91(5)	0.89(4)	2.2(1)	*0.4(5)*	0.7(1)	–	32	19
A-CH-D1	2.54(3)	2.98(7)	0.90(3)	0.95(3)	1.06(2)	2.57(6)	*0.3(3)*	0.9(1)	–	16	6
A-Ch-D2	0.639(6)	2.7(1)	0.87(4)	0.96(3)	0.65(6)	1.8(2)	*0.0(4)*	0.5(1)	–	95	37
L-Ch-A	0.47(2)	7.9(5)	0.89(3)	0.98(2)	n.m.	n.m.	*1(1)*	n.m.	n.m.	24	n.m.
L-Ch-B	1.59(8)	4.9(3)	0.84(2)	0.93(2)	n.m.	n.m.	*0.1(7)*	n.m.	n.m.	63	n.m.
L-Ch-C	0.80(4)	4.5(3)	0.82(5)	0.89(5)	n.m.	n.m.	*0.1(9)*	n.m.	n.m.	68	n.m.
L-Ch-D1	0.64(3)	4.9(3)	0.87(5)	0.94(4)	0.42(9)	0.9(2)	*0.3(9)*	*0.1(2)*	–	52	76
L-Ch-D2	0.65(3)	2.9(2)	0.85(6)	0.89(5)	1.4(1)	2.2(2)	*0.2(6)*	1.1(2)	–	67	28
L-Ch-D3	0.83(4)	4.9(3)	0.82(4)	0.91(4)	0.46(6)	1.0(1)	*0.0(9)*	0.2(1)	–	89	62
L-Ch-D4	2.915(5)	4.38(7)	0.84(2)	0.91(2)	0.56(6)	1.1(1)	*0.0(5)*	0.3(1)	–	58	29
L-Ch-E1	1.113(5)	2.78(8)	0.81(3)	0.92(3)	0.63(5)	1.2(1)	*–0.1(4)*	0.3(1)	–	100	27
L-Ch-E2	0.724(5)	4.9(1)	0.90(3)	0.96(2)	1.36(9)	3.1(3)	*0.3(6)*	1.2(2)	–	34	14
L-Ch-E3	0.598(5)	6.2(2)	0.90(3)	0.94(2)	0.5(1)	1.5(3)	*0.4(7)*	0.3(2)	–	28	42
L-Ch-E4	0.785(5)	5.6(1)	0.84(2)	0.94(3)	1.0(3)	1.6(6)	*0(7)*	0.7(4)	–	100	21
L-Ch-E5	0.656(5)	6.3(2)	0.87(2)	0.93(2)	0.56(9)	1.1(2)	*0.2(8)*	0.3(2)	–	46	44
L-Ch-E6	0.316(5)	6.5(4)	0.84(5)	0.92(4)	0.7(2)	2.2(6)	*0(1)*	0.6(3)	–	93	43
L-Ch-E7	3.700(5)	3.64(6)	0.83(1)	0.93(1)	0.25(2)	1.17(8)	*–0.1(4)*	0.12(5)	–	45	35
L-Ch-F	2.197(5)	5.0(1)	0.83(2)	0.92(2)	0.55(2)	0.98(4)	*–0.2(6)*	0.2(1)	–	35	32
L-Ch-G	1.616(5)	4.2(1)	0.87(2)	0.95(2)	1.04(3)	0.98(3)	*0.1(5)*	0.4(2)	–	32	20
L-Ch-H	2.037(5)	4.0(3)	0.90(3)	0.94(3)	1.00(5)	1.8(1)	*0.3(6)*	0.7(2)	–	15	12
R-Ch35-A	1.042(2)	3.64(9)	1.03(4)	0.83(3)	1.17(3)	2.75(9)	0.9(4)	1.0(1)	1.2(6)	8	6
R-Ch35-B	0.984(9)	2.49(9)	1.6(1)	0.84(7)	0.76(2)	1.34(4)	1.3(4)	0.4(1)	0.3(1)	6	14
R-Ch36-D	0.240(2)	2.4(3)	0.8(1)	0.8(1)	0.82(7)	3.9(5)	*–0.1(9)*	0.8(1)	–	100	26
R-Ch37-C	0.718(9)	2.56(8)	0.98(5)	0.89(4)	0.55(5)	1.4(1)	0.5(4)	0.3(1)	0.7(7)	15	39
S-Ch-A	2.828(7)	3.65(5)	1.02(2)	0.90(2)	0.52(3)	1.5(1)	0.8(4)	0.3(1)	0.4(2)	4	11
S-Ch-B	3.063(3)	3.52(5)	0.91(1)	0.86(1)	2.05(2)	2.75(3)	0.5(4)	1.8(2)	4(3)	9	3
S-Ch-C	2.290(7)	3.48(8)	0.87(2)	0.90(2)	3.31(3)	3.58(4)	*0.1(4)*	3.1(4)	–	40	2
S-Ch-D	3.301(3)	3.38(4)	0.87(1)	0.86(2)	2.87(3)	3.20(5)	*0.1(4)*	2.6(3)	–	22	3
S-Ch-E	1.283(7)	4.12(9)	1.12(3)	0.87(2)	5.30(6)	4.01(5)	1.2(5)	5.1(6)	4(2)	10	3
S-Ch-F	0.79(2)	4.5(2)	1.18(3)	0.84(3)	1.07(4)	1.73(6)	1.4(6)	0.8(2)	0.5(2)	5	10
S-Ch-G	0.651(3)	4.9(2)	1.47(8)	0.79(4)	68.1(6)	5.23(5)	2.3(6)	68(7)	{29(8)}	7	0
S-Ch-H1	0.350(9)	4.8(3)	1.05(8)	0.80(4)	23.0(6)	5.03(8)	1.3(8)	23(3)	{17(10)}	16	2

Table A1. Ne and Ar isotopic and elemental compositions, $^{20}Ne_{tr}$, $^{36}Ar_{tr}$ concentrations, and $(^{36}Ar/^{20}Ne)_{tr}$ ratios of Allende, Leoville, Renazzo, Semarkona, Bishunpur, and Krymka chondrules. Also given are blank contributions to $^{20}Ne_{tr}$ and $^{36}Ar_{tr}$ concentrations (%).[a] *Continued.*

Sample[b]	Weight (g) $\times 10^{-4}$	^{20}Ne	$^{20}Ne/^{22}Ne$	$^{21}Ne/^{22}Ne$	^{36}Ar	$^{36}Ar/^{38}Ar$	$^{20}Ne_{tr}$	$^{36}Ar_{tr}$	$(^{36}Ar/^{20}Ne)_{tr}$[c]	Blank contr. to $^{20}Ne_{tr}$	Blank contr. to $^{36}Ar_{tr}$
S-Ch-H2	0.29(1)	3.8(2)	0.90(8)	0.89(8)	3.1(2)	4.2(3)	*0.4(9)*	3.0(4)	–	31	17
S-Ch-I	0.23(2)	4.9(5)	0.96(9)	0.84(7)	3.9(4)	4.1(5)	*1(1)*	3.7(7)	–	5	18
S-Ch-K	0.148(8)	2.9(4)	0.8(1)	0.78(9)	0.9(2)	2.3(6)	*0(1)*	0.7(3)	–	100	55
B-Ch-A (PP)	2.98(1)	3.75(6)	0.84(2)	0.91(3)	2.00(3)	5.9(1)	*0.1(4)*	2.0(2)	–	48	1
B-Ch-A2 (PP)	1.37(4)	3.5(1)	0.86(3)	0.88(3)	1.40(5)	3.5(1)	*0.1(5)*	1.3(2)	–	45	10
B-Ch-B (POP)	1.58(1)	4.27(9)	1.06(3)	0.90(2)	1.75(3)	2.40(5)	1.1(4)	1.5(2)	1.4(6)	12	7
B-Ch-C (CC)	1.61(1)	4.30(9)	1.06(4)	0.84(3)	0.13(4)	0.4(1)	1.2(5)	*–0.11(7)*	–	12	100
B-Ch-D (RP)	1.51(1)	3.85(8)	0.93(3)	0.89(3)	0.25(2)	0.75(6)	0.6(5)	*0.0(1)*	–	15	56
B-Ch-E (P)	0.81(3)	3.3(2)	0.90(4)	0.91(4)	1.5(1)	2.4(2)	*0.2(5)*	1.3(3)	–	36	15
K-Ch-A	1.9(1)	8.9(5)	0.87(3)	0.92(2)	n.m.	n.m.	*0(1)*	n.m.	n.m.	16	n.m.
K-Ch-B	0.786(5)	9.0(2)	0.80(2)	0.91(2)	1.93(2)	1.18(1)	*0(1)*	1.0(3)	–	100	21
K-Ch-C	0.677(5)	8.7(2)	0.84(2)	0.93(2)	3.12(3)	1.60(1)	*0(1)*	2.1(4)	–	100	8
K-Ch-D1	2.43(3)	9.8(2)	0.85(1)	0.91(2)	2.05(5)	1.38(3)	*0(1)*	1.2(3)	–	53	5
K-Ch-D2	1.64(3)	9.8(2)	0.86(1)	0.92(2)	1.24(5)	0.94(3)	*1(1)*	0.4(2)	–	9	25

[a]Gas concentrations are given in units of 10^{-8} cm^3STP/g. The numbers in parentheses ( ) represent uncertainties (1σ) in units of the least significant digit. The cosmogenic correction of the measured ^{20}Ne and ^{36}Ar ($^{20}Ne_{tr}$, $^{36}Ar_{tr}$) is explained in the text. $^{20}Ne_{tr}$ and $^{36}Ar_{tr}$ values in italics equal zero within uncertainties.

[b]For Bishunpur, chondrule types could be specified from a thin section that mirrored the sample slice from which the chondrules were separated; PP = porphyry pyroxene, POP = porphyry olivine pyroxene, CC = cryptocrystalline, RP = radial pyroxene. All other chondrules are mostly of the porphyry type.

[c]$(^{36}Ar/^{20}Ne)_{tr}$ ratios are given for samples with $^{20}Ne_{tr}$ and $^{36}Ar_{tr}$ above zero within uncertainties. For numbers in brackets { }, contamination with matrix material during sample separation cannot be excluded; n.m. = not measured.

Table A2. Ne and Ar isotopic and elemental compositions, $^{20}Ne_{tr}$, $^{36}Ar_{tr}$ concentrations, and $(^{36}Ar/^{20}Ne)_{tr}$ ratios of Renazzo, Semarkona, Bishunpur, and Krymka metal-sulfide-rich samples. Also given are proportions of blanks to the $^{20}Ne_{tr}$ and $^{36}Ar_{tr}$ concentrations (%).[a]

Sample	Weight (g) $\times 10^{-4}$	^{20}Ne	$^{20}Ne/^{22}Ne$	$^{21}Ne/^{22}Ne$	^{36}Ar	$^{36}Ar/^{38}Ar$	$^{20}Ne_{tr}$	$^{36}Ar_{tr}$	$(^{36}Ar/^{20}Ne)_{tr}$	Blank contr. to $^{20}Ne_{tr}$	Blank contr. to $^{36}Ar_{tr}$
R-MSC-A	1.55(3)	2.5(1)	1.6(1)	0.75(5)	3.31(7)	3.85(6)	1.3(2)	3.13(8)	2.4(4)	3	4
R-MSD-B	0.29(2)	4.0(4)	7(3)	0.5(2)	1.2(2)	1.8(2)	3.8(6)	0.9(2)	0.24(5)	6	41
R-MSD-C	2.344(8)	1.37(3)	4.4(4)	0.52(6)	1.53(2)	1.98(4)	1.22(9)	1.17(3)	0.96(7)	2	5
R-MSD-D	2.550(3)	2.02(6)	5.5(4)	0.47(4)	0.79(1)	1.21(4)	1.9(1)	0.44(2)	0.24(2)	1	5
S-MS-A	0.541(7)	9.0(3)	3.4(2)	0.60(3)	230(4)	5.35(6)	7.5(6)	229(4)	30(1)	1	0.1
S-MS-B	0.34(1)	8.6(5)	3.5(3)	0.51(5)	144(5)	5.32(6)	7.4(8)	144(5)	19(1)	5	0.3
S-MSC-A	1.36(2)	6.4(1)	2.49(7)	0.65(2)	122(2)	5.30(4)	4.8(4)	122(2)	25.2(8)	2	0.1
B-MSC-A	1.42(2)	5.4(2)	2.3(1)	0.70(3)	160(2)	5.32(4)	3.9(6)	159(2)	41(6)	1	0.1
B-MSC-F	1.96(6)	7.4(3)	2.50(7)	0.75(2)	99(3)	5.26(4)	5.3(7)	98(3)	18(2)	1	0.1
K-MSC-B	0.861(5)	8.9(2)	1.31(4)	0.80(2)	146(1)	5.17(4)	3.8(4)	145(1)	38(4)	7	0.1
K-MSC-D	0.466(5)	12.3(4)	1.33(5)	0.86(3)	127(1)	5.12(4)	5.1(7)	126(2)	25(3)	6	0.2
K-MSC-E	0.84(3)	7.4(3)	0.86(3)	0.93(2)	4.7(2)	2.49(6)	0.0(4)	3.9(2)	[b]	76	7
K-MSC-F	0.32(2)	9.8(6)	1.65(7)	0.87(4)	199(11)	5.17(6)	5.1(5)	198(11)	39(4)	5	0.5
K-MSC-G	0.54(2)	12.1(5)	1.63(6)	0.85(3)	188(5)	5.14(5)	6.4(6)	187(5)	29(3)	1	0.1

[a]Gas concentrations are given in units of 10^{-8} cm^3STP/g. The numbers in parentheses ( ) represent uncertainties (1σ) in units of the least significant digit. The cosmogenic correction of the measured ^{20}Ne and ^{36}Ar ($^{20}Ne_{tr}$, $^{36}Ar_{tr}$) is explained in the text.

[b]No $(^{36}Ar/^{20}Ne)_{tr}$ ratio can be given because no $^{20}Ne_{tr}$ is detected.